WSRC-TR-2003-00574
SRT-RPP-2003-00252

Determination of Cesium (Cs^+) Adsorption Kinetics and Equilibrium Isotherms from Hanford Waste Simulants using Resorcinol-Formaldehyde (RF) Resins (U)

March 2004

Savannah River Technology Center

SRS savannah river site™

WSRC-TR-2003-00574
SRT-RPP-2003-00252

KEYWORDS:
Hanford River Protection Project
Ion-exchange
Kinetics
Equilibrium
Cesium
Resorcinol-Formaldehyde Resins
RETENTION - Permanent

Key WTP R&T References:

Test Specification:
24590-PTF-TSP-RT-03-006

Task Plan:
WSRC-TR-2003-00257

Test Exceptions:
24590-WTP-TEF-RT-03-064
24590-WTP-TEF-RT-04-00009

R&T Focus Area:
Alternative Cesium Ion Exchange

Test Scoping Statement:
A-207

Determination of Cesium (Cs^+) Adsorption Kinetics and Equilibrium Isotherms from Hanford Waste Simulants using Resorcinol-Formaldehyde Resins (U)

SAVANNAH RIVER TECHNOLOGY CENTER

William D. King
Cheryl E. Duffey
Stephen H. Malene

Publication Date: March 2004

Westinghouse Savannah River Company
Savannah River Site
Aiken, SC 29808

Prepared for the U.S. Department of Energy Under Contract Number DE-AC09-96SR18500

SRS savannah river site ™

This page was intentionally left blank

TABLE OF CONTENTS

LIST OF TABLES

LIST OF FIGURES

(This Page Intentionally Left Blank)

TABLE OF NOTATION

c_i	Initial Cs^+ liquid-phase concentration, [M]
c_f	Final Cs^+ liquid-phase concentration, [M]
m_i	Mass of filter-dried resin, (g)
F	F-factor for conversion from filter-dried to oven-dried resin mass, (-)
K_d	Chord of isotherm at an equilibrium liquid-phase Cs^+ concentration level
Q	Cesium loading on resin, mmol Cs/g of dry resin
T	Liquid-phase temperature (contact temperature), ºC
ϕ	Phase ratio (liquid-to-resin), ml of solution/gram of dry resin
$\rho_{skeletal}$	Skeletal density of resin (g/mL)
M_R	Mass of dry resin (g)
M_{P+L}	Mass of pycnometer and liquid (g), (without added resin)
M_{P+L+R}	Mass of pycnometer, liquid, and resin (g)
ρ_L	Density of liquid (g/mL)

1.0 Testing Summary

This report describes the results of cesium sorption kinetics and equilibrium isotherm tests with resorcinol-formaldehyde (RF) resin using Tank AN-105 simulated waste. These tests were conducted at the Savannah River Technology Center (SRTC) in support of the Hanford River Protection Project - Waste Treatment Plant (RPP-WTP). The RPP-WTP contract was awarded to Bechtel for the design, construction, and initial operation of a plant for the treatment and vitrification of millions of gallons of radioactive waste currently stored in tanks at Hanford, WA. A crucial part of the current treatment process involves the removal of cesium from waste tank supernate solutions using columns containing SuperLig® 644 resin. Due to concerns about the chemical and hydraulic performance of SuperLig® 644 resin in large-scale operations, RF resin was evaluated as a potential alternative to the baseline material. Extensive testing was conducted at Pacific Northwest National Laboratory (PNNL) on various RF samples (both granular and spherical) obtained from different vendors. Three RF samples (two spherical and one granular) were subsequently delivered to SRTC based on initial screening results at PNNL, which indicated good performance for these materials. A small number of tests were then conducted at SRTC on the RF resin using non-radioactive simulant solutions to support development of a preliminary column performance model.

1.1 Objectives

Test Objective	Objective Met (Y/N)	Discussion
A data set that characterizes the impact of particle size and temperature on particle kinetics under loading conditions.	N/Y	Test Exception 24590-WPT-RT-04-00009 eliminated particle size testing. The baseline form chosen was of uniform size thus, particle size studies were not needed. Results for temperature dependent kinetics work are described in Section 4.1.
A data set that characterizes the impact of temperature and nitric acid concentration on particle kinetics under elution conditions.	N	Test Exception 24590-WPT-RT-04-00009 eliminated testing under elution conditions. WTP-R&T indicated other testing showed excellent elution performance for spherical RF and this work was no longer required.
A data set that characterizes the impact of Na^+, K^+, Cs^+, and OH^- concentrations on equilibrium under loading conditions.	Y	Results described in Section 4.2
Cesium equilibrium data under nominal elution conditions.	N	Test Exception 24590-WPT-RT-04-00009 eliminated testing under elution conditions. WTP-R&T indicated other testing showed excellent elution performance for spherical RF and this work was no longer required.

1.2 Test Exceptions

Test Exception	Description
24590-WTP-TEF-RT-03-064	The test exception changed the sodium concentration to be used for off-nominal testing with AN-105 simulant from 4 M to 6 M Na^+.
24590-WTP-TEF-RT-04-00009	The test exception eliminated all elution (acid side) testing. Particle size testing was also eliminated with the change of the baseline material from granular to mono-disperse spherical. Scope was increased to include testing of the spherical and granular materials.

1.3 Results and Performance Against Success Criteria

Success Criteria	Results and Performance
Determination of pore diffusivity based on particle kinetics under loading and elution conditions.*	Kinetics tests conducted with a differential column test apparatus provided reproducible and accurate cesium uptake data versus time for resorcinol-formaldehyde resin. The data indicates that the cesium sorption rate is quite fast with essentially complete equilibrium being attained between the liquid and solid phases within 48 hours for both RF resin forms. "True" equilibrium loading values were confirmed in these tests by extending the contact times to 72 hours. There was no indication of resin degradation or displacement of cesium by slower sorbing competitors during this time frame at 25 °C. Cesium equilibrium loading data for each sample tested in the differential column are provided in Table 1-1. Essentially no difference was observed in the results for used and unused spherical resins. The equilibrium loading value obtained for granular RF at 6.65 μg Cs/L (average) was 16% higher than the value obtained for spherical RF at the same initial concentration. The equilibrium loading value obtained for SuperLig® 644 was 32% higher than the value obtained for spherical RF. Kinetics test results (normalized with regard to maximum loading) obtained at 25 °C for spherical RF (used and unused), granular RF, and for a -20/+30 mesh sample of granular SuperLig® 644 resin are provided in Figure 1-1. Cesium sorption rates for the samples tested varied in the sequence: spherical RF > granular RF > SuperLig® 644. However, the sorption rates for all three resin types are similar and appear to be suitable for the intended application. Normalized (with regard to maximum loading) temperature-dependent data for the spherical RF resin is provided in Figure 1-2. As expected, the cesium sorption rate increases and the equilibrium loading decreases with temperature (Table 1-1). Cesium loading (at the maximum) on RF resin decreased by 17% when the temperature was increased from 25 to 45 °C. In addition, the 45 °C test showed a decrease in loading after 8 hours. This may indicate degradation of the resin at elevated temperatures.

Success Criteria	Results and Performance
Determination of cesium equilibrium distribution coefficient values over the range of expected resin loading and elution conditions.**	Batch contact tests conducted with the spherical RF resin provided reproducible results that were consistent with the equilibrium data obtained by the kinetics test method with this material. Table 1-2 provides equilibrium loading data obtained for RF resin during batch contact testing. The four-point cesium sorption isotherm obtained for spherical RF resin with AN-105 simulant is shown in Figure 1-3 along with the isotherm obtained for SuperLig® 644 resin (-20 to +30 mesh) in the same simulant. The total cesium capacities of the two materials are comparable as indicated by the maximum loading values observed (estimated total cesium capacities: spherical RF – 0.49 mmol Cs/g resin, SuperLig® 644 – 0.54 mmol Cs/g resin; see Hamm, 2004).The differences in curvature of the RF and SuperLig® 644 isotherms are likely due to the different selectivities of the two materials for cesium over the other competitor ions. RF resin is less selective than SuperLig® 644 resin for cesium over the other competitors. One cesium equilibrium data point for spherical RF resin is included in Figure 1-3 that was obtained by the kinetics test method. The consistency of the RF equilibrium loading data obtained by the two test methods is confirmation of equilibrium data accuracy for both methods. Equilibrium data obtained for the modified AN-105 simulants is provided in Figure 1-4. The impacts of varying the concentrations of Na^+, K^+, and OH^- (or, conversely H^+) on cesium equilibrium loading are evident and the data trends are generally as expected. Cesium loading levels on RF resin increase as Na^+, K^+, and H^+ ion concentrations decrease. Similar trends in cesium loading have been observed for SuperLig® 644 resin using the same modified AN-105 simulants (Hamm, 2004). Equilibrium loading values observed at higher cesium concentrations near the upper ends of the isotherms ranged from 0.32 to 0.42 mmol Cs/g resin, with the extreme values being associated with the high and low potassium simulants, respectively. This indicates that potassium is the competitor of greatest significance within the range of waste feed compositions.

*The kinetics test data satisfied the intended objectives of the Task Plan and was provided to the individuals responsible for the determination of cesium pore diffusivity values and ultimately for the generation of a RF column transport model.

**The equilibrium loading data satisfied the intended objectives of the Task Plan and was provided to the individuals responsible for the calculation of rational selectivity coefficients and the generation of a multi-component isotherm model.

1.4 Quality Requirements

This work was performed in accordance with the RPP-WTP QA requirements specified for work conducted by SRTC as identified in DOE IWO M0RSLE60. SRTC has provided matrices to WTP demonstrating compliance of the SRTC QA program with the requirements specified by WTP. Specific information regarding the compliance of the SRTC QA program with RW-0333P, Revision 10, NQA-1 1989, Part 1, Basic and Supplementary Requirements and NQA-2a 1990, Part 2.7 is contained in these matrices.

This work was conducted according to the QA requirements in Test Specification 24590-PTF-TSP-RT-03-006, Rev. 0 (Abodishish, 2003) and Task Plan WSRC-TR-2003-00257, Rev. 0 (Duffey, 2003b). This work was not required to comply with RW-0333P, Rev. 10. This work does comply with NQA-1 1989, Part 1, Basic and Supplementary Requirements and NQA-2a 1990, part 2.7.

1.5 R&T Test Conditions

Test Conditions	Conditions Followed? (Y/N)
Simulants – Approved standard AN-105 simulant will be used during testing. Modified AN-105 simulants will also be used to accommodate variations in OH^-, K^+, and Na^+ concentrations. Nitric acid solutions (concentrations to be determined) will be used during acid side testing.	Y/N Test Exception 24590-WPT-RT-04-00009 eliminated testing under elution (acid side) conditions. WTP-R&T indicated other testing showed excellent elution performance for spherical RF and this work was no longer required.
Resin Sampling and Pretreatment – The baseline RF resin produced by separate supplier for PNNL testing and provided to SRTC under separate task shall be used for the cesium ion exchange tests. The 6-liter batch of potassium form RF resin is the baseline material and will be shipped to SRTC under an inert gas in a tightly closed container. The lot number, date of receipt, treatment of the resin, and general storage conditions prior to use will be recorded and reported.	Y/N Test Exception 24590-WPT-RT-04-00009 changed the baseline material to a spherical form. WTP-R&T indicated the spherical form had better characteristics.
Physical Properties – In support of modeling efforts, key physical resin properties will be measured. These properties include particle size distribution, porosities, and densities.	Y
Batch Contact Protocol – Prior to initiation of batch contact testing, a standard test protocol must be developed and verified. Parameters such as contact times and agitation rates must be optimized to ensure and adequate approach to equilibrium. Particle kinetics testing will be used for protocol verification.	Y

Test Conditions	Conditions Followed? (Y/N)
Particle Kinetics – Particle kinetics testing under loading conditions will be conducted at 25 °C using unsieved resin and up to three resin sieve fractions. One additional test using unsieved resin will be performed at an elevated temperature. A testing method will be developed for particle kinetics under elution conditions. One test will be conducted using unsieved resin under nominal temperature and acid conditions. An additional test varying temperature or acid concentration will be performed.	Y/N Test Exception 24590-WPT-RT-04-00009 changed the baseline material to a mono-disperse spherical resin and eliminated testing under elution (acid side) conditions. WTP-R&T indicated other testing showed excellent elution performance for spherical RF and this work was no longer required.
Batch Contact Equilibrium Testing – Batch contact testing will be conducted using unsieved resin at 25 °C. Data will be obtained with AN-105 simulant for the purpose of developing the cesium loading isotherm. Additional testing will include variations in Na^+, K^+, and OH^- concentrations. Impacts of these variables on the cesium loading isotherm will be addressed. A testing method will be developed for batch contact testing under elution conditions using resin that has been previously loaded with cesium. One test will be conducted using unsieved resin under nominal temperature and acid conditions	Y/N Test Exception 24590-WPT-RT-04-00009 eliminated testing under elution (acid side) conditions. WTP-R&T indicated other testing showed excellent elution performance for spherical RF and this work was no longer required.

1.6 Simulant Use

Only AN-105 simulants were used for this body of work. No results are available for actual waste testing. Conclusions are not dependent upon the use of actual waste, but are solely a measure of resin performance.

1.7 Discrepancies and Follow-on Tests

No issues of plant significance were identified in this work and no follow-on tests are planned.

Table 1-1. Cesium equilibrium loading levels as determined by kinetics testing of Resorcinol-Formaldehyde and SuperLig® 644 resins at the point of maximum loading.

Simulant Batch[a]	Temperature (°C)	Particle Type (resin)	Cs Loading[b] (mmol/g)
Batch 2	25	Used Spherical (RF)	1.01E-01
Batch 2	45	Used Spherical (RF)	8.39E-02
Batch 2	25	Unused Spherical (RF)	1.01E-01
Batch 2	25	Unused Granular (RF)	1.17E-01
Batch 1[c]	25	Used Spherical (RF)	1.28E-01
Batch 1	25	Used Spherical (RF)	1.30E-01
Batch 1[d]	25	Used Spherical (RF)	1.23E-01
Batch 1	25	Unused Granular (SuperLig® 644)	1.72E-01

[a] Batch 1 c_i $(Cs)_{avg}$ = 5.90E-04 M, Batch 2 c_i $(Cs)_{avg}$ = 5.00E-04 M
[b] Mass basis is dry sodium form resin. Maximum loading at 30 mL/min (12.5 cm/min) unless otherwise indicated.
[c] Flow rate = 90 mL/min (37.5 cm/min)
[d] Flow rate = 0.5 mL/min (0.208 cm/min)

Table 1-2. Cesium equilibrium loading isotherm data for Resorcinol-Formaldehyde and SuperLig® 644 resins with nominal and modified AN-105 simulants.

Simulant Type	Liquid-Phase Equilibrium [Cs] (M)	Solid-Phase Equilibrium Cs Loading[a] (mmol Cs/g resin)
Spherical RF Resin		
Nominal	1.15E-05	0.0120
Nominal	5.44E-05	0.0414
Nominal	5.77E-04	0.1786
Nominal	1.98E-03	0.3714
Low OH^-	1.23E-05	0.0144
Low OH^-	2.89E-03	0.3213
High OH^-	1.01E-05	0.0129
High OH^-	1.77E-03	0.4065
Low K^+	2.20E-06	0.0159
Low K^+	1.82E-03	0.4173
High K^+	3.95E-05	0.0114
High K^+	3.09E-03	0.3296
High Na^+	1.57E-05	0.0128
High Na^+	2.37E-03	0.3304
SuperLig® 644 Resin		
Nominal	3.31E-06	0.0163
Nominal	1.85E-05	0.0656
Nominal	2.03E-04	0.2488
Nominal	8.40E-04	0.4767

[a] Mass basis is dry sodium form resin

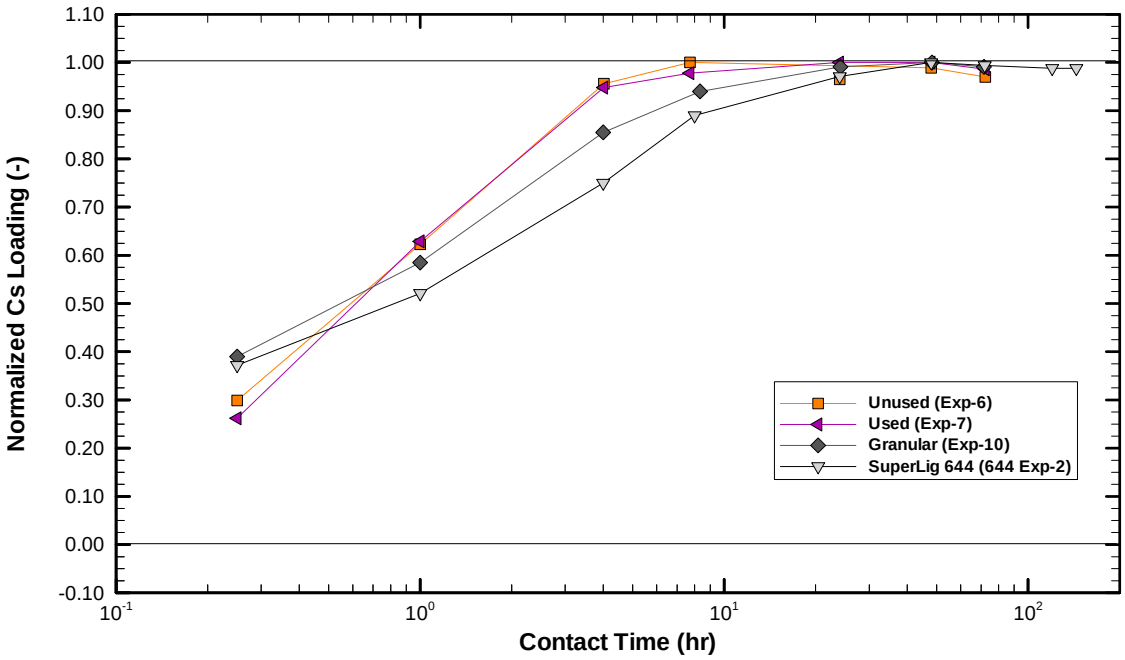

Figure 1-1. Normalized transient Cs loading levels for used and unused spherical RF, granular RF and granular SuperLig® 644. Normalized = (mmol Cs/g)/(mmol Cs/g at maximum).

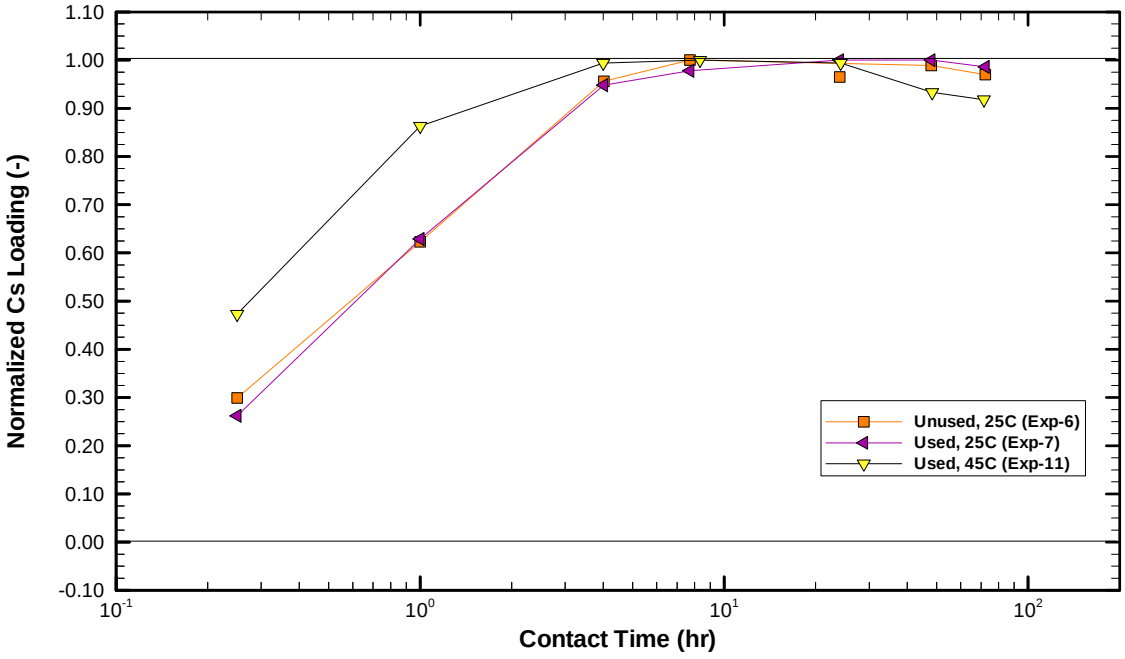

Figure 1-2. Normalized transient cesium loading levels for spherical RF at the two temperatures studied. Normalized = (mmol Cs/g)/(mmol Cs/g at maximum).

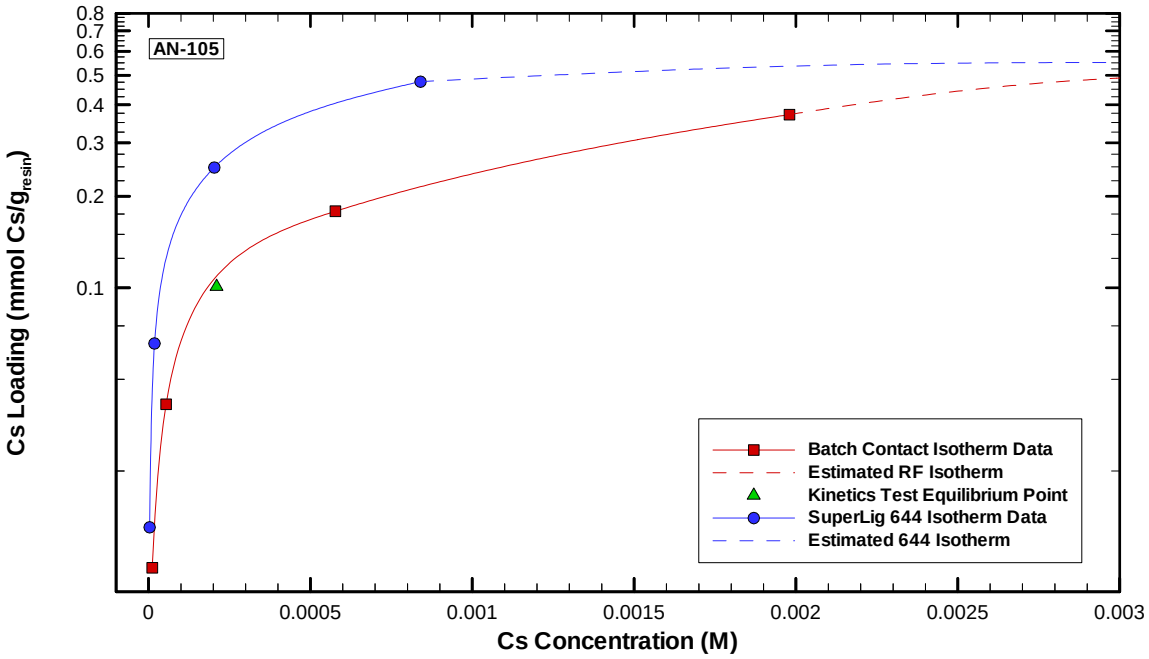

Figure 1-3. Cesium sorption isotherms for spherical RF and granular SuperLig® 644 resins with AN-105 simulant.

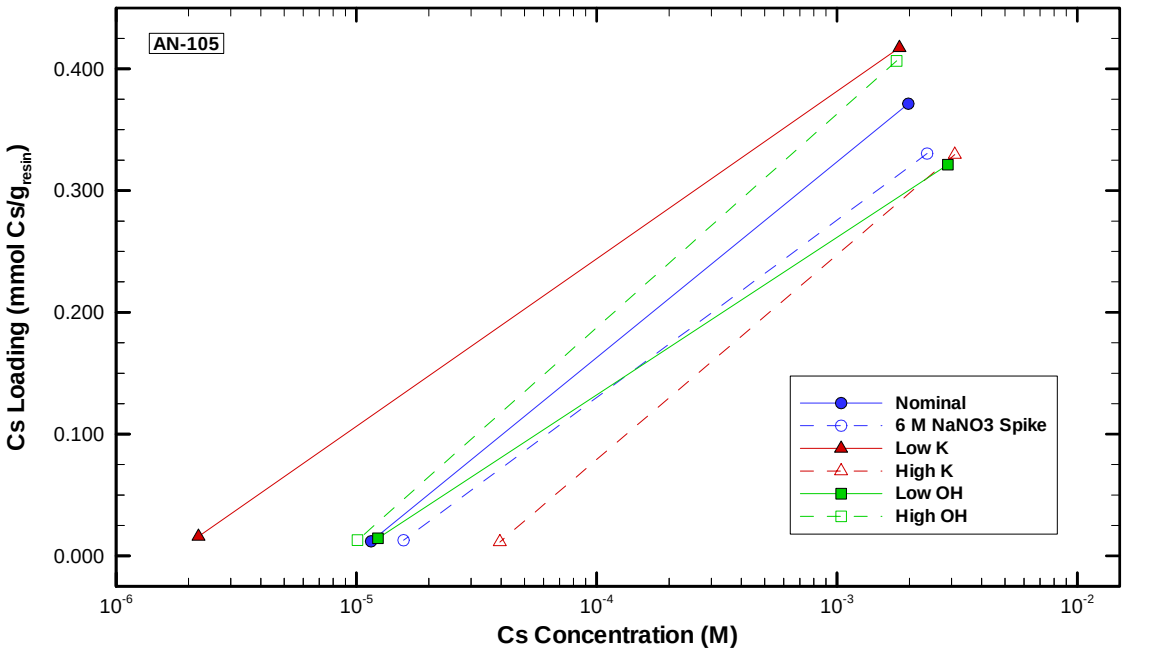

Figure 1-4. Cs isotherm endpoint data for spherical RF resin using modified AN-105 simulants.

2.0 Background and Introduction

Millions of gallons of radioactive waste were produced as a by-product of the production of nuclear weapons at various government sites across the United States. The current legacy waste inventory has essentially been reduced to two main sites (Hanford, WA and Aiken, SC) which are currently managed by the Department of Energy. Separate waste treatment processes have been developed for each site due to differences in waste composition and regulatory requirements for ultimate disposal. Development of the Hanford waste treatment strategy was originally contracted to BNFL, Inc. Based on limited initial testing and extensive nuclear waste processing experience, a treatment process was developed that included the following basic steps: 1) separation of low volume, high activity solids from high volume, lower activity supernate, 2) treatment of the supernate for the removal of specific radionuclides (strontium, transuranics, and cesium) using precipitation and ion-exchange technologies, 3) evaporation of the bulk decontaminated low activity supernate, 4) vitrification of the decontaminated and concentrated supernate to generate low activity waste glasses, and 5) vitrification of high activity solids and ion-exchange eluate solutions to generate concentrated high activity glasses. This treatment scheme was designed to minimize the volume of high activity waste requiring disposal.

Extensive testing was conducted in support of the original BNFL design for the Hanford waste treatment plant at the Savannah River Technology Center (SRTC) in Aiken, SC and at Pacific Northwest National Laboratory (PNNL) in Hanford, WA, during the period from 1998 - 2001. The test results indicated that the conceptual design plan was adequate and the Department of Energy subsequently contracted Bechtel to design, build, and perform initial operations of the waste treatment plant at Hanford. The River Protection Project - Waste Treatment Plant (RPP-WTP) for treatment of the Hanford radioactive waste is currently under construction. Design validation and process optimization tests continued at SRTC and at PNNL during the final design and initial construction phases from 2001 - 2003.

The initial plant treatment schedule focuses on 10 waste storage tanks located at Hanford which have been categorized into four general waste types (or Envelopes). Envelopes A - C refer to liquid supernate samples that vary in chemical composition, while Envelope D refers to solids (sludge) primarily isolated from tank heels. Extensive testing has been conducted on actual samples in each waste category that were retrieved from the tanks. In order to minimize costs associated with sample isolation, transfer, and handling, recipes have been developed at SRTC and PNNL to prepare nonradioactive simulants of various tank samples based on analysis data from actual samples. Supernate simulants have been developed for several specific waste tanks and are being used for testing throughout the RPP-WTP test program. All tank supernate compositions are dominated by sodium salts (dominant counterions: nitrate, nitrite, hydroxide, and aluminate), which are generally present in high concentrations (2 - 10 M Na^+). All waste samples are highly caustic. Minor waste constituents are extensive in number and type and the targeted radionuclides for removal are present at concentrations that are several orders of magnitude lower than the concentrations of the primary constituents. These conditions require treatment technologies that are highly selective. The baseline pretreatment methodology for the supernate involves evaporation or dilution to near 5 M Na^+ followed by precipitation and

filtration for removal of radioactive strontium and transuranic elements (only needed for Envelope C) and ion-exchange treatment for the removal of cesium. The design ion exchange process for cesium removal involves the use of multiple large columns in a sequential carousel configuration with off-line column elution and regeneration.

SuperLig® 644 resin is the chosen technology for removal of radioactive Cs-137 from Hanford waste supernates. SuperLig® 644 is a proprietary, granular, organic resin that undergoes significant shrink/swell volume changes under column loading and elution conditions. SuperLig® 644 is a high cost resin that is solely available through IBC Advanced Technologies, Inc. Furthermore, in 2002, pilot-scale tests conducted at SRTC with the baseline resin revealed high pressure drops across SuperLig® 644 columns during transitional phases of the design chemical processing sequence. The Department of Energy (DOE), Office of River Protection (ORP) directed Bechtel National Incorporated (BNI) to initiate a three step process for selection and potential implementation of an alternative ion exchange resin for cesium removal in the RPP-WTP. BNI completed the first step of this process with the recommendation that RF be pursued as a potential alternative to the contract-specified SuperLig® 644 for cesium removal (Thorson, 2003).

The resorcinol-formaldehyde resin used in this test was prepared by condensation polymerization of resorcinol and formaldehyde. The resin has been shown to be highly selective for cesium removal in caustic, high sodium solutions including actual Hanford waste samples. Cesium primarily exists in the aqueous supernate as the dissociated ion, Cs^+. Competitor ions for exchange with RF resin are believed to include Na^+, K^+, and H^+, as is the case for SuperLig® 644 resin (Hamm, 2000). Under column loading conditions with 5 M Na^+ solutions, it is believed that the primary bound species is sodium ion and cesium sorption primarily involves the exchange of sodium and cesium ions. Potassium ion is a significant competitor and cesium selectivity over potassium is a primary factor determining the overall effectiveness of a given technology for cesium removal with these waste types. H^+ ion is a minor bound species under column loading conditions with highly caustic supernates. Conversely, under acidic column elution conditions (likely 0.5 M HNO_3 in the plant process), H^+ ion is the primary bound species and rapidly displaces the other bound ions from the resin upon acid contact. It should be emphasized that RF resin also undergoes volume changes during transitions between the sodium and hydrogen forms. As a result, the granular form of this material may be expected to perform similarly to SuperLig® 644 resin in large-scale operations. However, the relatively low compressibility and regular shape of the spherical RF resin may lead to superior hydraulic flow properties and large-scale chemical performance.

A primary tool for evaluating the viability of RF resin as an alternate cesium removal technology in the RPP-WTP is a preliminary column performance model under development at SRTC. The overall objective of the model is to predict the chemical performance of RF resin in large-scale plant operations with a range of liquid feed compositions. Data requirements of the column transport model have been discussed in detail elsewhere (Hamm, 2000; Duffey, 2003a) and are briefly summarized below. The baseline liquid processing flow rate for plant column operations (3 BV/hr, where 1 BV = the volume of processed liquid equivalent to the resin bed volume) is believed to be sufficiently fast that sorption kinetics would significantly impact the shapes of the RF column cesium breakthrough profiles during loading. Therefore, experimental determination

of the fundamental diffusional parameters (as described by film and pore diffusion coefficients) impacting cesium sorption kinetics with RF resin is important for accurate column performance modeling. Another fundamental requirement for accurate modeling with variable feed compositions is the measurement of cesium adsorption isotherms for numerous representative liquid-phase compositions and the determination of selectivity coefficients for the various competitor species. Certain resin physical properties (i.e. particle size, density) are also required by the model as well as carefully measured properties of the packed resin bed (i.e. geometry, void, etc.). Finally, column performance data collected under prototypical processing conditions is needed for confirmation of the predictive capabilities of the model. This report summarizes recent kinetics, equilibrium, and physical properties data obtained for RF resin with baseline and modified AN-105 simulants. Extensive column tests were conducted at PNNL with various RF resin samples and these results are reported elsewhere (Fiskum, 2004). The collective data obtained at both SRTC and PNNL will be utilized to develop and verify the column transport model.

3.0 Experimental

3.1 Resin History and Handling

3.1.1 Resin History

One granular and two spherical samples of RF resin were received for testing from PNNL in 2003. The majority of the spherical RF resin received had previously been used in compressibility testing at PNNL and is referred to as "used". Unless indicated, all experiments were conducted with the "used" resin. A small sample of "unused" spherical RF resin was also received and served as a control. The spherical resin samples were received in polyethylene bottles as dry hydrogen form material under nitrogen. The spherical samples tested were obtained from production Batch #1 (equivalent to Battelle batch ID #3, (Fiskum, 2004)). The granular material was received, unused, in the potassium form. The test sample was a composite of production batches BCS-187-1-0002 (6 L batch) and BCS-187-4-0001 (600 g batch) (equivalent to Battelle batch ID #9, (Fiskum, 2004)). The combined resin was split several times using a sample splitter to produce representative 1-L sub-samples. The samples were placed in polyethylene bottles and the headspace above the bottles was purged with nitrogen before capping. One such bottle was delivered to SRTC for column (Hassan, 2003) and kinetics testing.

3.1.2 Resin Conditioning and Sampling

Each resin sample was sequentially pretreated as follows: 0.5 M HNO_3 acid (10 BV in 2 portions over 2 - 3 hours), water (10 BV in 2 portions over 1 hour), 1.0 M NaOH (10 BV in 2 portions over 2 - 3 hours), and water (10 BV in 2 portions over 1 hour) in a 1 L beaker. This pretreatment cycle was then repeated a second time. The pH of the final slurry was adjusted to 12 with 0.1 M NaOH solution to ensure that the resin was in the sodium form. After several hours the pH was checked and adjusted again as needed. The conditioned sample slurries were stored in closed polyethylene bottles in pH 12 solution.

The used, spherical RF resin was utilized for numerous tests. The pretreated material was split into several portions using a simple glass sampling tube prior to testing (1-in. ID). Each sampling event involved the collection and compositing of multiple (at least three) vertical core sub-samples after some initial tumbling of the storage bottle to mix the material. 1-inch or 1.5-cm ID sampling tubes were used depending on the sample size needed. The pretreated sample was split into several 50 - 100 mL samples in this manner and provided to individual researchers for kinetics, batch contact, drainable void and skeletal density testing. This sampling method followed an established procedure used throughout the ion exchange testing program at SRTC (King, 2003).

For chemical performance tests (kinetics and batch contact) individual test samples were subsequently isolated as described below. Resin mass measurements for specific tests were conducted following an established protocol (King, 2003). Dry mass determination involved rapid removal of free-flowing liquid from the resin by filtration under an argon blanket, followed by essentially simultaneous collection of a damp test sub-sample and multiple small (0.1 g)

samples for the determination of water content. The test samples were typically re-wetted immediately after damp weight measurement. Water content was determined by drying known masses of damp resin in a vacuum oven (45 °C, -30 in. Hg) until a constant weight was obtained. A weight correction factor (F-factor) was calculated for determination of the dry mass of the actual test sample. The F-factor was defined as the resin dry mass divided by the damp mass. Table 3-1 details sodium-form F-factor data for all kinetics experiments.

Some tests with spherical RF resin utilized sodium-form resin for the initial state of the resin while others used hydrogen-form material. In order to evaluate the collective data, a mass conversion factor was needed for the two resin forms. The resin I-factor is defined as the mass ratio of sodium to hydrogen forms. Since sodium is heavier than hydrogen one would expect the mass of sodium-form resin to be higher and the I-factor to be larger than one. Two methods were utilized to measure the I-factor for spherical RF resin. In each case the initial state of the resin was sodium form stored at pH 12. Method 1 involved weighing a sodium-form resin sample in the damp state along with four F-factor samples that were dried to determine the sample dry-sodium mass. The damp test sample was then converted to the hydrogen form using 0.5 M HNO_3 and washed with water until the cover liquid pH was stable at 3. The liquid was removed from the sample and the entire sample was dried to determine the dry hydrogen-form mass. The I-factor measured by Method 1 was 1.235. Method 2 involved completely drying a sample of sodium-form resin to determine the dry sodium mass. The sample was then rehydrated in water and converted to the hydrogen form as described above prior to drying to determine the dry hydrogen mass. The I-factor measured by Method 2 was 1.218. The average I-factor determined by the two methods was then 1.226 with a standard deviation of 0.012.

3.2 Simulant Preparation and History

Sodium hydroxide solutions utilized for testing were prepared from NaOH pellets and filtered prior to use. Deionized (Millipore®) water was used for all reagent preparations. All simulant solutions were prepared according to procedures published by Eibling (2001). The simulant recipe was based on analysis data for actual samples collected from Hanford waste tank 241-AN-105. Reagent grade chemicals were utilized for all preparations. The concentrations of selected species added during initial simulant preparation based on the recipe are provided in Table 3-2. This table also provides the average measured concentrations of selected species in the baseline AN-105 simulant. Modified simulants were prepared as above with varying concentrations of Na^+, K^+, NO_3^-, and OH^-. The target and measured concentrations of these species are given in Table 3-3.

3.3 Equipment and Procedure

3.3.1 Sorption Kinetics Testing

The kinetics experimental setup was based upon a differential column concept described in detail previously (Duffey, 2003a). This concept dictates utilization of a thin resin bed exposed to a feed solution with nearly uniform uptake being observed throughout the bed. In essence, this setup was designed to determine resin adsorption properties of a differential cross-sectional area of a typical column during operation. Implementation of this concept required a controlled flow

of liquid through the resin bed, a controlled temperature throughout the system, and continuous homogenization of the liquid phase. A schematic of the kinetics experimental setup is shown in Figure 3-1. Targeted experimental variables are given in Table 3-4. The jacketed differential column was constructed by the SRTC glass blowers specifically for this task. Prior to assembly of the apparatus the damp resin test sample was placed in the containment reservoir. The resin was held in place between two 100-mesh stainless steel screens. Void space within the apparatus was filled with 1-mm glass beads to minimize dead-space. The simulant was fed through the column in upflow to minimize the amount of air initially in the system. An argon sparge was continually supplied to the feed. The system remained closed with the exception of a small vent/sampling port as described below. The resin bed path length and diameter were 5.4 mm and 17.5 mm respectively, giving a resin volume near 1.3 mL (assuming complete packing of the containment reservoir).

The simulant feed was held within a capped 125-mL polyethylene bottle and was continually stirred with a 1-inch PTFE stir bar. 0.5 mL samples were withdrawn from the bottle at 15 minutes, 1-, 4-, 8-, 24-, 48-, and 72-hours using a 5-mL plastic syringe fitted with a 4-inch #18 stainless steel needle. Earlier experiments included a 120-hour sample. The feed bottle was contained within a jacketed glass beaker containing water for temperature control. Most experiments were conducted using a Cole-Parmer gear pump with PEEK gears, a stainless steel head, and PTFE seals. Gear pumps were chosen to deliver a smooth, pulseless flow. The low-flow experiment was conducted with a Stepdos reduced pulsation diaphragm-metering pump with a PVDF head, FFPM valves and gaskets, and PTFE-coated diaphragm. Calibration curves depicting the flow rate of water (mL/min) versus pump setting were generated for all pumps prior to kinetics experimentation.

The differential column and jacketed beaker temperatures were controlled using a Haake DC-5 recirculating unit. The column and beaker were attached in series with the inlet from the recirculator entering the bottom of the beaker and the outlet returning to the recirculator from the top of the column. A Neslab Cool Flow CFT-33 chiller was attached to the recirculating unit to help maintain the recirculator temperature in the 25 °C experiments. Scoping experiments indicated there was significant heat loss from the simulant through the stainless steel pump heads at 45 °C. To eliminate this problem the pump heads were wrapped with a 4’x 1/4” heat tape controlled by an attached mini-controller. The heat tape was wrapped with insulating web and held in place with heat resistant tape. Heat loss was minimized in the 25 °C experiments by wrapping the stainless steel pump heads with insulating web held in place by heat resistant tape. The simulant temperature within the column was monitored using a metal thermometer (with digital display) inserted through the top of the column to a point just above the resin bed.

The general experimental procedure is described below. The simulant was filtered just prior to testing using a 0.45 μm Nalgene® filter cup and samples were collected for analyses. The simulant was weighed into a 125 mL polyethylene bottle yielding 120 mL of feed solution. A PTFE stir bar was added, and the bottle was capped. The jacketed beaker was placed on a stir plate. A chiller set at 15°C was attached to the recirculator for the 25 °C experiments. The recirculator was set to yield the appropriate temperature and the water flow was initiated. The simulant bottle was placed in the jacketed beaker and water was added to the beaker to simulant level. The argon and outlet lines were installed at a level above the feed line intake to avoid

aspirating gas into the liquid feed intake. Argon flow was initiated that yielded on average 2 - 3 mm bubbles at a flow rate of approximately 150 - 200 bubbles/min. Stirring was initiated within the simulant bottle and the column and the simulant were equilibrated to the experimental temperature. Adjustments were continually made during experiments to fine-tune the temperature of the simulant as it passed through the resin bed. The pump was turned on and timing was initiated when the simulant made contact with the resin bed. Weights of each sample and the temperature of the simulant at each sampling were recorded. The outlet (return) line was then removed from the simulant bottle and an effluent flow rate verification was performed using a graduated cylinder and stopwatch.

3.3.2 Batch Contact Equilibrium Testing

Batch contact equilibrium tests were conducted in an orbital shaker oven (Innova 4230). Each test sample contained 1.000 +/- 0.002 g (dry mass) of Na-form resin and 100 +/- 2 mL of simulant. The samples were placed in 250-mL polyethylene bottles that were sealed with rubber septa. The bottles were purged with argon for 10 - 15 minutes and then placed on the shaker table in a horizontal orientation. The agitation rate was set to 100 RPM and the oven was maintained at 25 +/- 0.5 °C throughout the test. This agitation rate and bottle orientation were selected based on the belief that sample agitation was adequate to reach full equilibrium between the liquid and solid phases without causing significant physical degradation to the resin particles. The samples were agitated for a total of 48 hours based on preliminary tests that confirmed attainment of equilibrium under these conditions within this time period. The bottles were inspected twice each day to confirm that all resin particles were immersed in the solution. Bottles were rotated longitudinally as needed to wash any resin particles back into the solution that were stuck to the bottle above the solution. The number of resin particles not immersed at any point was typically less than five. At the conclusion of the tests the samples were removed from the oven and filtered through 0.45 um Nalgene nylon disposable filter units. Sub-samples of the filtrate were then submitted for cesium analysis by ICP-MS. Analytical results and masses for individual samples used are provided in the Appendix.

3.3.3 Physical Properties Testing

3.3.3.1 Skeletal Density Determination

A sample of preconditioned Na-form spherical RF resin was isolated using the core sampling method. Half of the sample was converted to the H-form using 0.5 M HNO_3. The Na- and H-form portions of the resin were then dried to a constant weight in a vacuum oven at 45 °C and –30 inches Hg for skeletal density determination. The method used roughly followed ASTM D 854 – 02. The skeletal density of the resin in Na-form was determined in DI H_2O and baseline AN-105 simulant. The skeletal density of the resin in H-form was determined in DI H_2O and 0.5 M HNO_3. All measurements were taken using ~25 mL glass pycnometers. The dry mass of each pycnometer (including the lid) was obtained. The mass of the pycnometer and indicated liquid was obtained as follows. The pycnometer was filled near the top with the indicated liquid, the lid pushed on tightly, all the liquid wiped from the outside of the vessel, and the vessel was then weighed. When wiping the lid, special care was taken not to wick any liquid from the top. Care was also taken not to warm the pycnometer by excessive rubbing or handling. Once the mass

was obtained the liquid was removed from the pycnometer. Approximately one gram of the indicated dry resin was weighed into the appropriate pycnometer. The pycnometer was filled ¾ full with the indicated liquid and the vessel was gently agitated to remove entrapped air. A small piece of parafilm was placed over the top and the resin was allowed to rehydrate overnight. The pycnometer was then filled near the top and the above procedure followed to determine the mass of the pycnometer, liquid, and resin. The density of each liquid was then determined by weighing an exact volume.

The skeletal density was calculated for each sample as follows:

$$\rho_{skeletal} = \frac{M_R}{M_{P+L} - (M_{P+L+R} - M_R)} \times \rho_L$$

where

$\rho_{skeletal}$	-	skeletal density of resin (g/mL)
M_R	-	mass of dry resin (g)
M_{P+L}	-	mass of pycnometer and liquid (g), (without added resin)
M_{P+L+R}	-	mass of pycnometer, liquid, and resin (g)
ρ_L	-	density of liquid (g/mL)

3.3.3.2 Drainable Void Determination

The drainable void volume of a spherical RF resin bed packed in a prototypical manner (see reference procedure, Steimke, 2003) was determined by a liquid drainage technique. An apparatus was constructed and the method was refined using 1-mm diameter borosilicate glass beads as a surrogate for the resin. The apparatus consisted of a clear plastic tube (1-inch ID, 1/8-inch wall) approximately twelve inches long (Figure 3-2). The tube was mounted vertically at eye level by means of a stainless steel block with internal manifolds accommodating an in-line drain valve and a de-ionized water supply valve at a right angle. The tube was sealed into the block with an o-ring and set screws. A fine mesh stainless steel screen was supported by three one-sixteenth inch by one-eighth inch stainless steel bars evenly spaced across the diameter at the bottom end of the tube within the block. Two viewing slots were machined into the valve block below the screen level to facilitate the observation of water flow.

The top of the tube was opened for filling with resin. A tight fitting rubber stopper with a central one-quarter inch diameter hard walled plastic tube that served as an air supply line was used to blow air down through the resin bed. This was done to ensure the complete capture of all of the water held within the voids during the drainage for subsequent weighing. The supply air was fully saturated with water by flowing through a large six-inch diameter quarter-inch wall clear acrylic pipe approximately six feet tall, maintained to a level approximately half full of water. From the laboratory air compressor, the air was regulated to no more than 20 psig, and then controlled with a needle valve into the bottom of the water column. The air outlet at the top of

the water column was directed through a tee fitting through another needle control valve into a rotometer type flow meter and finally ending through the stopper at the top of the measurement column. The other air path through the center of the tee fitting was piped into a twelve foot vertical u-tube, half full of water, that served as a pressure relief valve and a visual air pressure gauge. The saturated air was blown down through the sample column only with the drain valve in the open position and the collection beaker in place. The airflow was set to approximately one scfm for two-minute time intervals. The intervals were repeated until the weighing results stabilized. This maximum cumulative weight was used directly to relate to the void space in the test column media.

The maximum experimentally achievable void fraction for a packed bed of mono-sized spheres is 36.4% assuming no ordering, particle deformation, or wall effects. Deviation from a mono-modal distribution often leads to higher packing density and lower bed voidage (German, 1989).

Results of drainable void tests using 1-mm glass beads are given in Table 3-5. After subtracting the weight of the volume of water below the screen (41.85 grams) and converting the weight of the water into equivalent volume, the average void space of the three runs through the glass beads was 33.71 mL void per 100 mL bed (33.7% porosity of glass beads, +/- 1%). This data demonstrated good reproducibility and reasonable results for this test method.

3.3.4 Analysis Methods and Instrumentation

3.3.4.1 ADS Analysis

Simulant samples were submitted to the SRTC Analytical Development Section (ADS) for analysis. Analysis methods included Inductively Coupled Plasma – Mass Spectroscopy (ICP-MS), Inductively Coupled Plasma-Emission Spectroscopy (ICP-ES), Ion Chromatography-Anion (IC Anion), and Microtrac® particle size analysis. Quality assurance and control procedures and blank and standard results for each analysis set are documented and maintained by ADS and are not reported here.

3.3.4.2 Supporting Equipment and Additional Analysis

Digital balances and temperature probes used during experimentation were calibrated by the SRTC Standards Laboratory. The balance calibration was checked in the laboratory prior to use each day. Simulant densities were determined by measuring the weight of 100 or 250 mL of solution at ambient temperature in the appropriate volumetric flask.

Table 3-1. F-factor values of Na-form RF resins used in kinetics experiments based on oven- and filter-dried resin masses.

Kinetics Experiment [a]	Experiment Date	Particle Type	F-factor
Experiments 1/2[b]	09/25/03	Used, spherical	0.4376
Experiment 3	10/22/03	Used, spherical	0.4101
Experiment 4	10/04/03	Used, spherical	0.4445
Experiment 5	10/04/03	Unused, spherical	0.4762
Experiment 6	10/12/03	Granular	0.4817
Experiments 7	10/12/03	Used, spherical	0.4306

[a] F-factor determination was performed immediately prior to the kinetics experiment(s) indicated.
[b] Experiments 1 and 2 used resin from the same sub-sample of filter-dried resin. Thus, only one F-factor was performed.

Table 3-2. Target and measured concentrations of selected species in baseline AN-105 simulant.

Species[a]	Target Concentration (M)	Measured Concentration (M)
Na^+	5.000	5.068
K^+	0.090	0.093
Al[b]	0.687	0.502[c]
S[b]	0.004	0.004
P[b]	0.003	0.002
Cr[b]	0.012	0.011
B[b]	0.002	0.002
Si[b]	0.004	0.004
Nitrate	1.243	1.128
Nitrite	1.126	1.015
Sulfate	0.004	0.003
Phosphate	0.003	0.002
Chloride	0.120	0.113
Oxalate	0.003	0.002
Formate	0.030	0.025
Hydroxide	1.600	1.470[d]
Carbonate	0.098	NA

[a] Additional minor metals present at concentrations below 1.0 E-03 M include: Mg, Ca, Cd, Mo, Pb.
[b] Total elemental concentration including all species.
[c] [Al] consistently observed below AN-105 simulant target.
[d] Measured as free OH^-; (a portion of the OH^- is consumed by complexation with metals).

Table 3-3. Target and measured molar concentrations of selected species in nominal and modified AN-105 simulants with respective densities.

Simulant	$[Na^+]$ Target (Measured)	$[K^+]$ Target (Measured)	$[NO_3^-]$ Target (Measured)	$[OH^-]^a$ Target (Measured)	$[Al]^b$ Target (Measured)	Density (g/mL)
Nominal	5.00 (5.10)	0.09 (0.09)	1.24 (1.13)	1.60 (1.47)	0.69 (0.50)	1.225
Low OH	5.00 (5.20)	0.09 (0.10)	3.24 (3.23)	0.20 (0.21)	0.69 (0.00)[c]	1.246
High OH	5.00 (4.98)	0.09 (0.09)	0.75 (0.63)	2.00 (1.79)	0.69 (0.61)	1.220
Low K	5.00 (5.15)	0.00 (0.00)[d]	1.15 (1.13)	1.60 (1.22)	0.69 (0.50)	1.219
High K	5.00 (4.68)	0.70 (0.70)	1.85 (1.92)	1.60 (NA)	0.69 (0.50)	1.261
High Na concentrate	6.00 (6.07)	0.11 (0.11)	1.49 (1.69)	1.68 (1.91)	0.84 (0.68)	1.268
High Na spike	6.00 (5.80)	0.09 (0.09)	2.24 (2.19)	1.60 (1.53)	0.69 (0.50)	1.266

[a] Target values based on total added OH^-; analysis values represent free, uncomplexed hydroxide.
[b] Measured Al values consistently below targets; Al varied directly with OH^-.
[c] Al solubility very low with low OH^-, trace Al observed by analysis at 0.005 M.
[d] Some potassium added to simulant as molybdate salt; measured K^+ concentration: 0.002 M.

Table 3-4. Targeted experimental variables for kinetics testing using RF resins.

Kinetics Experiment [a]	Start Date	Particle Type	Temperature	Flow Rate (mL/min)	Simulant
Experiment 1	09/25/03	Used, spherical	25°C	90	Batch 1
Experiment 2	09/25/03	Used, spherical	25°C	30	Batch 1
Experiment 3	10/22/03	Used, spherical	25°C	0.5	Batch 1
Experiment 4	09/10/02	Used, spherical	25°C	30	Batch 2
Experiment 5	09/10/02	Unused, spherical	25°C	30	Batch 2
Experiment 6	09/17/02	Granular	25°C	30	Batch 2
Experiment 7	09/26/02	Used, spherical	45°C	30	Batch 2

Table 3-5. Drainable void data for 100 mL bed of 1-mm diameter glass beads.

Weighing Sequence	Trial #1 Drainage Wt. (g)	Trial #2 Drainage Wt. (g)	Trial #3 Drainage Wt. (g)
1	65.53	63.92	66.77
2	75.98	74.77	75.27
3	76.17	74.74	75.26
4	76.24	74.66	---
5	76.19	---	---

*100 ml of DI water weighs 99.16 grams

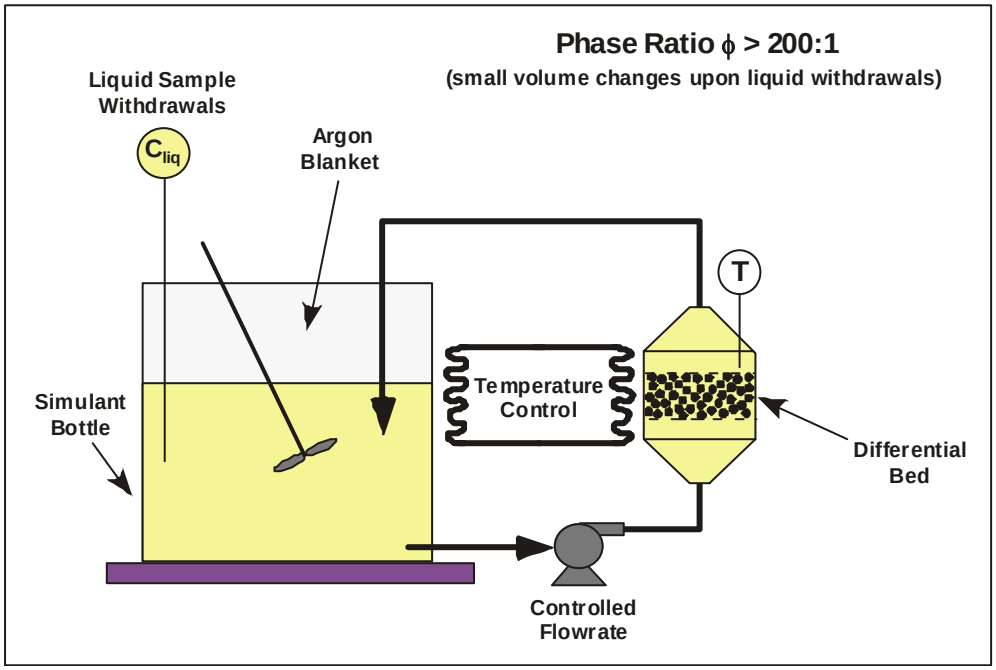

Figure 3-1. A simple schematic representation of the differential column and peripherals. The phase ratio is high and volume reductions due to liquid sample withdrawals are small.

Figure 3-2. Drainable void test apparatus.

4.0 Results and Discussion

4.1 Kinetics Testing

In total, seven kinetics experiments were performed. To reduce the total number of separate kinetics experiments required, a nominal set of testing conditions was chosen about which additional testing was performed by varying the key parameters such as temperature, particle type, and flow rate. The nominal testing conditions correspond to those used in Experiments 2 and 4, and are defined as: used spherical resin, 25 °C, and a 30 mL/min (12.5 cm/min) flow rate. All tests were performed using the same batch of "used" spherical RF resin with the exceptions of Experiment 5 (which was conducted using "unused" spherical RF resin) and Experiment 6 (which was conducted using granular RF resin). Experiments 1 - 3 were performed using Batch 1 AN-105 simulant with an average initial Cs concentration of 5.90E-04 M. Experiments 4 - 7 used Batch 2 AN-105 simulant with an average initial Cs concentration of 5.00E-04 M. All kinetic experiments were performed with an initial phase ratio greater than 200 in an attempt to minimize the impacts associated with the sampling withdrawals, each sample withdrawal being ~0.5 mL. Each kinetics test was operated with a total of 72 hours of simulant contact time with the exception of Experiments 1and 2, which lasted 120 hours. During the 3-day contact period, samples were withdrawn at the approximate time points: 0.25, 1, 4, 8, 24, 48, and 72 hours. All sample concentrations (including feed concentrations) were analyzed using ICP-MS. The early sampling times provide key information about the pore diffusion process, while the later sampling times provide information on the true equilibrium state. Cesium loading values were calculated from the ICP-MS data as follows:

$$Q = \frac{c_i - c_f}{F(m_i)}$$

where

- Q - Cs loading (mmol Cs/g resin)
- c_i - initial liquid-phase Cs concentration (M)
- c_f - final liquid-phase Cs concentration (M)
- F - resin F-factor (-)
- m_i - mass of filter-dried resin (g)

For comparison purposes, graphs showing the transient Cs loading levels and normalized Cs concentrations have been chosen. To better illustrate the early on kinetics aspect of each test, the graphs showing the normalized Cs concentrations are shown in semi-log scale.

To study the impact of contact temperature on the particle kinetics and equilibrium adsorption capacity, two separate kinetics experiments were performed (i.e., Experiments 4 and 5). The specific conditions of each temperature dependent kinetics test are listed in Table 4-1. Testing was performed at 25, and 45 ºC using the baseline Envelope A (AN-105) simulant. For the two experiments listed in Table 4-1, the measured liquid-phase Cs concentrations at the selected

sampling times are given in Table 4-2. Table 4-2 also provides the measured initial liquid-phase Cs concentrations, as well as the computed Cs loading and K_d values.

The computed Cs loading and normalized (with respect to maximum loading) concentration levels for each temperature dependent test are plotted in Figures 4-1 and 4-2, respectively. As expected and shown in Figure 4-1, the adsorption capacity of spherical RF resin drops at higher temperatures. A drop in capacity of approximately 17% was observed when the temperature was increased from 25 to 45 °C. Also, the results shown in Figure 4-1 indicate that no appreciable resin degradation (or slower competitor) effects are occurring in the 25 °C test as no decrease in capacity is observed. This indicates that a "true" equilibrium point on the appropriate adsorption isotherm has been measured. However, the same is not true in the 45 °C test. A decrease in the apparent capacity (maximum loading) of approximately 8% was observed between the 8- and 72-hour samples. This may indicate degradation of the resin at elevated temperatures.

To study the impact of particle type on the particle kinetics and equilibrium adsorption capacity, two additional kinetics experiments were performed (i.e., Experiments 5 and 6) using "unused" spherical resin and granular resin. The test conditions chosen were consistent with those of Experiment 4, with the exception of the variation in particle type. As the majority of testing within this work was to be performed using resin which had been previously used in compressibility testing, the test conducted with the "unused" resin provided a control to which other tests could be compared.

The specific conditions of each particle type dependent kinetics test are listed in Table 4-3. For the experiments listed in Table 4-3, the measured liquid-phase Cs concentrations at the selected sampling times are given in Table 4-4. Table 4-4 also provides the initial liquid-phase Cs concentrations, as well as the computed Cs loading and K_d values.

The computed Cs loading and normalized (with respect to maximum loading) concentration levels for each particle type dependent test are plotted in Figures 4-3 and 4-4, respectively. As shown in both figures, the rate of uptake and capacity for the "used" and "unused" spherical resins are virtually identical. The Cs loading rate for the spherical resin is slightly greater than that of the granular resin, with the granular exhibiting a greater capacity by approximately 16%.

The observed overall kinetics is established based primarily on the net result of mass transfer limitations at the particle level. Specifically, the overall mass transfer mechanisms of interest are: (1) film diffusion across the stagnant layer of liquid surrounding each individual particle, and (2) species molecular diffusion through the particle's pore structure. The particle's pore diffusion coefficients can be isolated for indirect measurement by increasing the rate of film diffusion based on increased liquid flow rate about the particles.

As indicated earlier, Experiment 2 (Batch 1 simulant) represents the nominal testing conditions. The flow rate for this experiment was 30 mL/min (i.e., a superficial velocity through the differential bed of ~12.5 cm/min). Previous work using SuperLig® 639 (Duffey, 2003a) and flow rates of 30, 60, and 90 mL/min confirmed that a 30 mL/min flow rate results in sufficiently high film mass transfer rates.

The specific conditions of each flow rate dependent kinetics test are listed in Table 4-5. In addition to tests at the nominal flow rate, testing was performed at flow rates of 90 mL/min (37.5 cm/min) and 0.5 mL/min (0.208 cm/min) using Batch 1 simulant. For the experiments listed in Table 4-5, the measured liquid-phase Cs concentrations at the selected sampling times are given in Table 4-6. Table 4-6 also provides the initial liquid-phase Cs concentrations, as well as the computed Cs loading and K_d values.

The computed Cs loading and normalized (with respect to maximum loading) concentration levels for each flow rate dependent test are plotted in Figures 4-5 and 4-6, respectively. As expected and shown in Figure 4-5, the adsorption capacity of used spherical RF is independent of flow rate. Only the time required to reach a true equilibrium value varies. (The 0.5 mL/min test appears to have a lower capacity but this is due to the lower measured initial Cs concentration.

Figures 4-5 and 4-6 illustrate there is only slight improvement in rate of Cs loading when the flow rate is increased from 30 to 90 mL/min. The impact of decreasing the flow rate is best illustrated by the normalized (with respect to maximum loading) Cs concentration curves shown in Figure 4-6. At the lowest flow rate (i.e., 0.5 mL/min, Experiment 3) the transport lag time associated with the connecting tubing within the kinetics apparatus is apparent at the first two sampling times.

4.2 Batch Contact Equilibrium Testing

Batch contact tests were performed with the spherical RF resin using the baseline AN-105 simulant and numerous modified AN-105 simulants. Table 4-7 provides the target concentrations for each component varied in the AN-105 simulant. The overall test matrix and simulant identification for the modified AN-105 simulants are provided in Table 4-8. Each of the modified AN-105 simulants was tested at the high and low cesium concentrations to obtain cesium sorption data near the isotherm endpoints. In general the concentrations selected for each of the three competitors for cesium sorption (Na^+, K^+, and H^+) were based on the known extreme concentrations for these species in the Hanford waste tanks. Therefore, the test matrix is believed to bracket the range of liquid phase compositions that might be experienced in the plant operation. Varying the concentrations of these species across such large ranges necessarily resulted in other, often undesired, changes to the matrix. For example, the simulants containing the highest concentrations of Na^+ and K^+ ion also had higher ionic strength and higher nitrate concentrations than the baseline simulant. Variation in the amounts of nitrate salts added during simulant preparation relative to the baseline recipe was the typical method utilized to modify the composition. Nitrate salts were selected as the primary varying species due to the belief that the nitrate ion concentration does not directly impact cesium sorption with RF resin. Another deviation from ideality resulted from the fact that the solubility of aluminum varies directly with the hydroxide concentration. As a result, the concentration of aluminum was observed to vary considerably in those simulants with off-nominal hydroxide levels, as shown in Tables 3-3 and 3-4.

The four-point cesium sorption isotherm obtained for the baseline simulant is shown in Figure 4-7 and the data is provided in Table 4-9. Based on the curvature of the isotherm, it is

apparent that the resin was not fully saturated at the highest cesium loading value, although the data does appear to approach the maximum loading for the resin in this matrix. The data fit indicates that the effective cesium loading capacity for spherical RF resin approaches 0.5 mmol Cs/g resin. The cesium loading value for spherical RF is ~90% (sodium form dry mass basis) of the loading capacity observed for SuperLig® 644 resin (0.54 mmol Cs/g resin) under the same conditions (Hamm, 2004). Relative performance on a per volume basis is obviously dependent upon the density differences between SuperLig® 644 and spherical RF. Although the capacity for RF resin is lower, this is likely sufficient capacity to meet the plant design requirements for cesium removal.

Two-point isotherm endpoint data was also obtained for the spherical resin with the modified AN-105 simulants. The data is provided in Table 4-9 and plotted in Figure 4-8. This data will be utilized along with the baseline data to generate continuous isotherm curves for each simulant composition. The isotherms will then be used to calculate rational selectivity coefficients and generate a multi-component isotherm model capable of predicting cesium uptake with RF resin for a wide range of liquid phase compositions. General trends observed in Figure 4-8 are consistent with those observed for SuperLig® 644 resin with the same simulants (Hamm, 2004). Cesium loading generally varied in the sequence: high K^+ < high Na^+ ≅ Low OH^- < nominal < high OH^- < low K^+.

Simulants M and N were unique relative to the other simulants in that all chemical components in the full AN-105 recipe were concentrated to 6 M Na^+. The cesium concentration extremes tested with this simulant were, however, the same as those used for the other simulants. Interest in testing an AN-105 simulant concentrate results from the fact that design personnel have considered plant operations with 6 M rather than 5 M Na^+ feed. However, direct evaluation of the resin performance with the 6 M Na^+ concentrate is not possible since the experimental design did not include the prototypical cesium concentration for this waste matrix. Analysis of spherical RF resin performance with 6 M Na^+ AN-105 concentrate will be performed during column transport modeling and will be reported separately.

4.3 Physical Property Testing

Results of the skeletal density testing of the used spherical RF are given in Table 4-10. The Na-form of the resin exhibited greater densities than did the H-form of the same resin. The skeletal densities of the Na- and H-forms in H_2O were greater than the densities in baseline AN-105 simulant and 0.5 M HNO_3, respectively. The same trend in skeletal densities was observed with SuperLig® 644 (Hamm, 2004).

Results of the drainable void tests are provided in Table 4-11. The drainable void fraction for a thirty-milliliter nominal sample of spherical RF resin was found to be 36.1% +/- 1%. Trial runs 1 and 4 were reasonably suspect and were omitted from this table and the final calculation. The weight of the volume of water below the screen (41.66 grams) must be subtracted from the maximum recorded weight of drainage for the void calculation to give the weight of water within resin bed. Temperature and density calibration corrections form the equivalent volume of void space in the column. The average void space through the resin is then 10.5 mL of void per 29.2 mL of resin bed (36.1% porosity of resin, +/- 1%).

Microtrac® analysis results for the used spherical and granular form of RF in sodium form are provided in the Appendix (Figures A-1 – A-4). The particle size distribution for the spherical material was quite narrow with the bulk of the distribution in the range 400 - 600 μm. The number-based mean of 458 μm was very near the volume-based mean of 486 μm, which is consistent with highly spherical particles with a narrow and symmetrical size distribution. In contrast, the number- and volume-based mean values obtained for the granular RF were 323 and 623 μm, respectively. Furthermore, the shapes of the number- and volume-based distributions were quite different. The number-based data indicates that the granular sample contains a significant number of fine particles.

Table 4-1. Experimental variables for temperature dependent kinetics testing using AN-105.

Variable		Experiment 4	Experiment 7
Start Date		10/04/03	10/12/03
Simulant		Batch 2	Batch 2
Avg. Temperature (°C)		25.1	44.3
Particle Type		Used Spherical	Used Spherical
Resin Dry Wt. (g)		0.3481	0.3367
Feed Volume (mL)		120	120
Phase Ratio (ϕ)		345	356
c_i (Cs)	**(μg/L)**	6.69E+04	6.60E+04
	(M)	5.03E-04	4.97E-04
Flow Rate	**(mL/min)**	30	30
	(BV/hr)	1385	1385
	(cm/min)	12.5	12.5

Table 4-2. Results summary for temperature dependent kinetics testing using AN-105 (Batch 2).

Experiment (T)	Time, t (hr)	Liquid Cs Concentration (c_f)		Loading, Q (mmol Cs/g resin)	K_d (mL/g)
		(μg/L)	(M)		
Experiment 4 (25°C)	0.00	6.69E+04	5.03E-04	0.00E+00	---
	0.25	5.67E+04	4.27E-04	2.65E-02	62
	1.00	4.24E+04	3.19E-04	6.35E-02	199
	4.02	3.00E+04	2.26E-04	9.57E-02	424
	7.72	2.88E+04	2.17E-04	9.88E-02	456
	24.00	2.79E+04	2.10E-04	1.01E-01	482
	48.00	2.79E+04	2.10E-04	1.01E-01	482
	72.35	2.85E+04	2.14E-04	9.96E-02	464
Experiment 7 (45°C)	0.00	6.60E+04	4.97E-04	0.00E+00	---
	0.25	5.12E+04	3.85E-04	3.97E-02	103
	1.00	3.90E+04	2.93E-04	7.24E-02	247
	4.00	3.49E+04	2.63E-04	8.34E-02	318
	8.33	3.47E+04	2.61E-04	8.39E-02	321
	24.17	3.49E+04	2.63E-04	8.34E-02	318
	48.33	3.68E+04	2.77E-04	7.83E-02	283
	71.53	3.73E+04	2.81E-04	7.70E-02	274

Table 4-3. Experimental variables for particle type dependent kinetics testing using AN-105.

Variable		**Experiment 4**	**Experiment 5**	**Experiment 6**
Start Date		10/04/03	10/04/03	10/12/03
Simulant		Batch 2	Batch 2	Batch 2
Avg. Temperature (°C)		25.1	25.3	24.9
Particle Type		Used Spherical	Unused Spherical	Granular
Resin Dry Wt. (g)		0.3481	0.3731	0.4001
Feed Volume (mL)		120	120	120
Phase Ratio (ϕ)		345	322	300
c_i (Cs)	**(μg/L)**	6.69E+04	6.69E+04	6.60E+04
	(M)	5.03E-04	5.03E-04	4.97E-04
Flow Rate	**(mL/min)**	30	30	30
	(BV/hr)	1385	1385	1385
	(cm/min)	12.5	12.5	12.5

Table 4-4. Results summary for particle type dependent kinetics testing using AN-105 (Batch 2).

Experiment (Sieve Fraction)	Time, t (hr)	Liquid Cs Concentration (c_f)		Loading, Q (mmol Cs/g resin)	K_d (mL/g)
		(μg/L)	(M)		
Experiment 4 (Spherical, used)	0.00	6.69E+04	5.03E-04	0.00E+00	---
	0.25	5.67E+04	4.27E-04	2.65E-02	62
	1.00	4.24E+04	3.19E-04	6.35E-02	199
	4.02	3.00E+04	2.26E-04	9.57E-02	424
	7.72	2.88E+04	2.17E-04	9.88E-02	456
	24.00	2.79E+04	2.10E-04	1.01E-01	482
	48.00	2.79E+04	2.10E-04	1.01E-01	482
	72.35	2.85E+04	2.14E-04	9.96E-02	464
Experiment 5 (Spherical, unused)	0.00	6.69E+04	5.03E-04	0.00E+00	---
	0.25	5.44E+04	4.09E-04	3.02E-02	74
	1.00	4.09E+04	3.08E-04	6.29E-02	204
	4.02	2.70E+04	2.03E-04	9.66E-02	475
	7.72	2.53E+04	1.90E-04	1.01E-01	529
	24.00	2.66E+04	2.00E-04	9.75E-02	487
	48.00	2.56E+04	1.93E-04	9.99E-02	519
	72.33	2.64E+04	1.99E-04	9.80E-02	493
Experiment 6 (Granular)	0.00	6.60E+04	4.97E-04	0.00E+00	---
	0.25	4.58E+04	3.45E-04	4.56E-02	132
	1.00	3.57E+04	2.69E-04	6.84E-02	255
	4.00	2.15E+04	1.62E-04	1.00E-01	621
	8.33	1.73E+04	1.30E-04	1.10E-01	844
	24.13	1.48E+04	1.11E-04	1.16E-01	1038
	48.25	1.43E+04	1.08E-04	1.17E-01	1084
	71.53	1.45E+04	1.09E-04	1.16E-01	1065

Table 4-5. Experimental variables for flow rate dependent kinetics testing using AN-105.

Variable		Experiment 1	Experiment 2	Experiment 3
Start Date		09/25/03	09/25/03	10/22/03
Simulant		Batch 1	Batch 1	Batch 1
Avg. Temperature (°C)		25.0	25.1	25.1
Particle Type		Used Spherical	Used Spherical	Used Spherical
Resin Dry Wt. (g)		0.3470	0.3469	0.3390
Feed Volume (mL)		120	120	120
Phase Ratio (ϕ)		346	346	354
c_i (Cs)	**(μg/L)**	8.10E+04	8.10E+04	7.69E+04
	(M)	6.09E-04	6.09E-04	5.79E-04
Flow Rate	**(mL/min)**	90	30	0.5
	(BV/hr)	4155	1385	23
	(cm/min)	37.5	12.5	0.208

Table 4-6. Results summary for flow rate dependent kinetics testing using AN-105 (Batch 1).

Experiment (Flow rate)	Time, t (hr)	Liquid Cs Concentration (c_f)		Loading, Q (mmol Cs/g resin)	K_d (mL/g)
		(μg/L)	(M)		
Experiment 1 (90 mL/min, 37.5 cm/min)	0.00	8.10E+04	6.09E-04	0.00E+00	---
	0.30	6.30E+04	4.74E-04	4.67E-02	99
	1.00	4.63E+04	3.48E-04	9.02E-02	259
	4.00	3.35E+04	2.52E-04	1.23E-01	490
	8.00	3.30E+04	2.48E-04	1.25E-01	503
	24.93	3.17E+04	2.39E-04	1.28E-01	538
	50.15	3.18E+04	2.39E-04	1.28E-01	535
	73.58	3.21E+04	2.42E-04	1.27E-01	527
	97.07	3.21E+04	2.42E-04	1.27E-01	527
	122.77	3.31E+04	2.49E-04	1.25E-01	500
Experiment 2 (30 mL/min, 12.5 cm/min)	0.00	8.10E+04	6.09E-04	0.00E+00	---
	0.20	6.81E+04	5.12E-04	3.34E-02	66
	1.02	5.06E+04	3.81E-04	7.90E-02	208
	4.00	3.36E+04	2.53E-04	1.23E-01	488
	8.00	3.21E+04	2.42E-04	1.27E-01	527
	24.92	3.11E+04	2.34E-04	1.30E-01	555
	50.15	3.25E+04	2.45E-04	1.26E-01	516
	73.45	3.20E+04	2.41E-04	1.27E-01	530
	96.95	3.44E+04	2.59E-04	1.21E-01	469
	122.73	3.21E+04	2.42E-04	1.27E-01	527
Experiment 3 (0.5 mL/min, 0.208 cm/min)	0.00	7.69E+04	5.79E-04	0.00E+00	---
	0.25	7.23E+04	5.44E-04	1.23E-02	23
	1.00	7.30E+04	5.49E-04	1.04E-02	19
	4.00	5.51E+04	4.15E-04	5.81E-02	140
	8.00	4.07E+04	3.06E-04	9.64E-02	315
	24.00	3.07E+04	2.31E-04	1.23E-01	533
	72.68	3.13E+04	2.35E-04	1.21E-01	516

Table 4-7. Target concentration levels for various species in AN-105 simulant matrix for batch contact equilibrium testing with RF resin.

Component	Low (M)	Nominal (M)	Intermediate (M)	High (M)	Base AN-105 Adjustments	Basis
Cs^+	1.58E-04	6.71E-04	2.65E-03	6.20E-03	varied $CsNO_3$ spike levels	values selected to determine full isotherm
K^+	0.00	0.09	---	0.7	varied KNO_3 spike levels	high value based on tank composition extreme
Na^+	---	5.0	---	6.0	concentration and spiking to 6 M Na^+	high/low values based on possible processing extremes
Free OH^-	0.2	1.4	---	2.0	exchanged $NaNO_3$ and NaOH to maintain $[Na^+]$	high/low values based on tank composition extremes

Table 4-8. AN-105 simulant matrix for batch contact equilibrium testing with spherical RF.

Simulant ID	Simulant Description	$[Cs^+]$	$[K^+]$	$[OH^-]$	Comments
A	Nominal	N	N	N	---
B	High Cs/Nominal	H	N	N	minimal variation in nitrate
C	Intermediate Cs/Nominal	I	N	N	minimal variation in nitrate
D	Low Cs/Nominal	L	N	N	minimal variation in nitrate
E	High Cs/ Low OH	H	N	L	low Al, high $[NO_3^-]$
F	Low Cs/ Low OH	L	N	L	low Al, high $[NO_3^-]$
G	High Cs/ High OH	H	N	H	low $[NO_3^-]$
H	Low Cs/ High OH	L	N	H	low $[NO_3^-]$[a]
I	High Cs/Low K	H	L	N	slightly lower $[NO_3^-]$
J	Low Cs/Low K	L	L	N	slightly lower $[NO_3^-]$
K	High Cs/High K	H	H	N	high $[NO_3^-]$
L	Low Cs/High K	L	H	N	high $[NO_3^-]$
M	High Cs/6 M Na^+ Concentrate	H	N	N	concentrated nominal recipe
N	Low Cs/6 M Na^+ Concentrate	L	N	N	concentrated nominal recipe
O	High Cs/6 M $NaNO_3$ Spike	H	N	N	spiking nominal to 6 M
P	Low Cs/6 M $NaNO_3$ Spike	L	N	N	spiking nominal to 6 M

Note: L = low, N = nominal, I = intermediate, H = high

Table 4-9. Cesium equilibrium loading isotherm data for baseline and modified AN-105 simulants with spherical RF resin.

Simulant	Liquid-Phase Equilibrium [Cs] (M)	Solid-Phase Equilibrium Cs Loading (mmol Cs/g resin)
A	1.15E-05	0.0120
B	5.44E-05	0.0414
C	5.77E-04	0.1786
D	1.98E-03	0.3714
E	2.89E-03	0.3213
F	1.23E-05	0.0144
G	1.77E-03	0.4065
H	1.01E-05	0.0129
I	1.82E-03	0.4173
J	2.20E-06	0.0159
K	3.09E-03	0.3296
L	3.95E-05	0.0114
M	2.16E-03	0.3881
N	1.16E-05	0.0194
O	2.37E-03	0.3304
P	1.57E-05	0.0128

Table 4-10. Skeletal densities of used spherical RF resin.

Sample	M_{P+L}	M_R	M_{P+L+R}	ρ_L	$\rho_{skeletal}$	Average $\rho_{skeletal}$
Na/H_2O-1	45.1571	0.8792	45.4947	0.9986	1.621	1.630
Na/H_2O-2	43.5738	0.8982	43.9246	0.9986	1.639	
Na/Sim-1	49.7788	0.9400	49.9867	1.2240	1.572	1.582
Na/Sim-2	49.7892	0.9572	50.0102	1.2240	1.591	
H/H_2O-1	44.3926	0.9463	44.7061	0.9986	1.493	1.490
H/H_2O-2	43.7031	1.3076	44.1325	0.9986	1.487	
H/HNO_3-1	44.2708	0.8007	44.5220	1.0113	1.474	1.471
H/HNO_3-2	45.1295	1.0907	45.4691	1.0113	1.469	

Table 4-11. Drainable void data for 29.2 mL bed of spherical RF resin.

Trial Number	Maximum Drainage Wt. (g)	Water Wt. from within Resin Bed (g)	Equivalent Volume of Bed Void Space (mL)
2	51.48	9.82	9.85
3	52.51	10.85	10.89
5	51.75	10.09	10.12
6	52.48	10.82	10.86
7	53.04	11.38	11.41
8	52.38	10.72	10.76

*100 ml of DI water weighs 99.6 grams

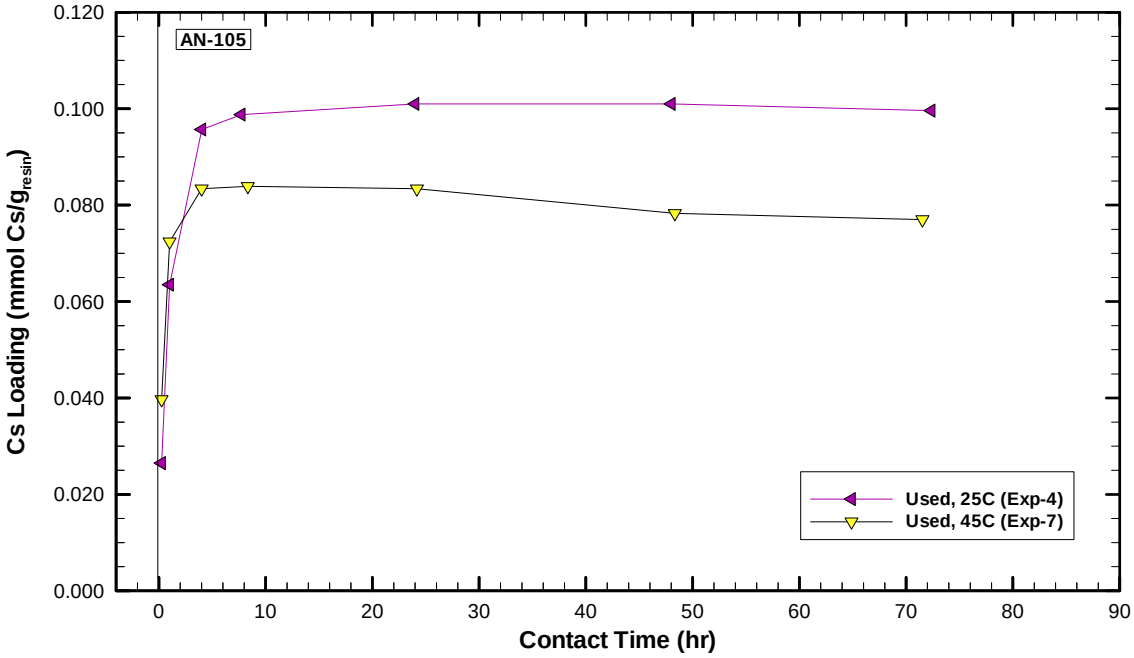

Figure 4-1. Transient Cs loading levels for the two contact temperatures studied.

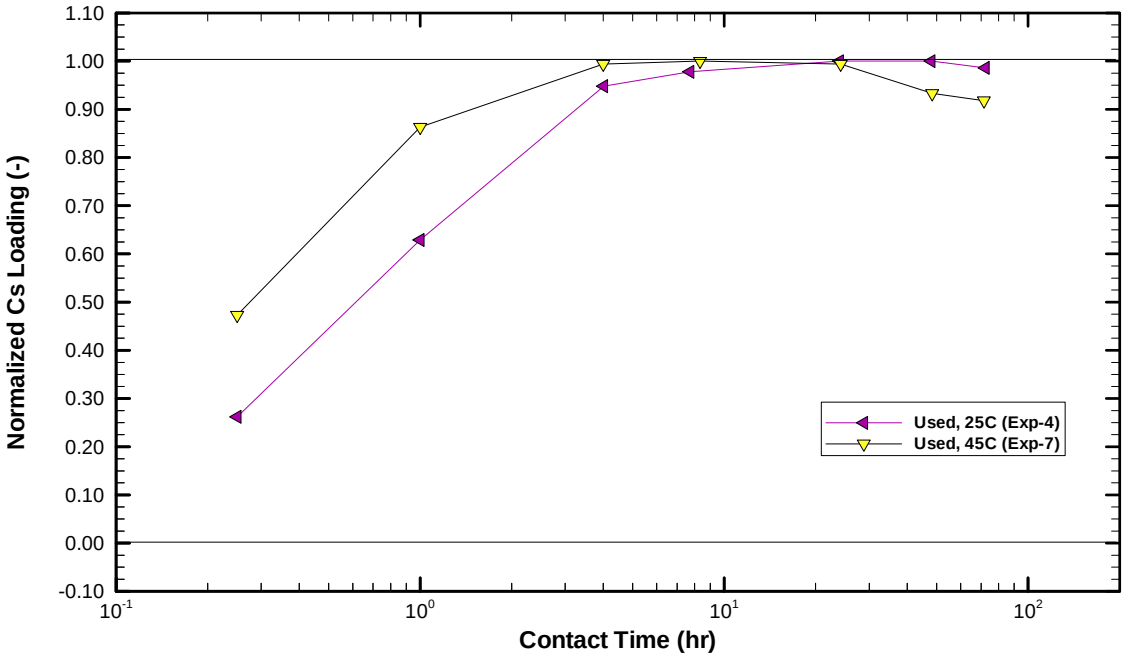

Figure 4-2. Normalized Cs concentration levels for the two contact temperatures studied.

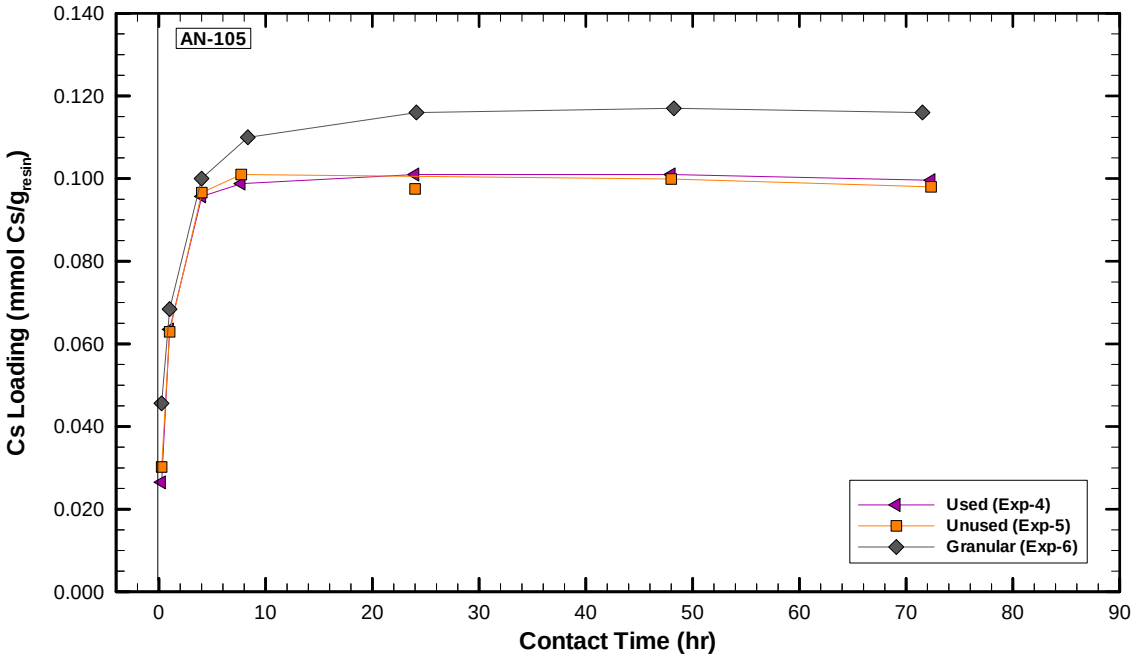

Figure 4-3. Transient Cs loading levels for the various particle types. Exp-4 and Exp-5 yield essentially the same curve indicating there is little difference in the behavior of the used and unused resins at 25 °C.

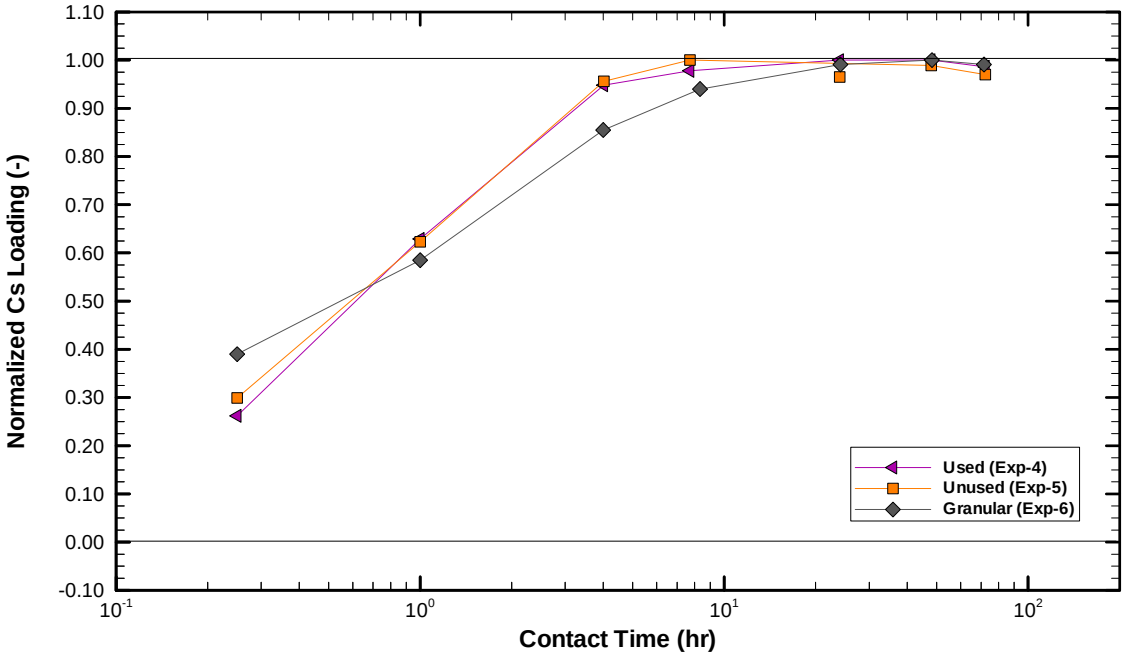

Figure 4-4. Normalized transient Cs concentration levels for the various particle types.

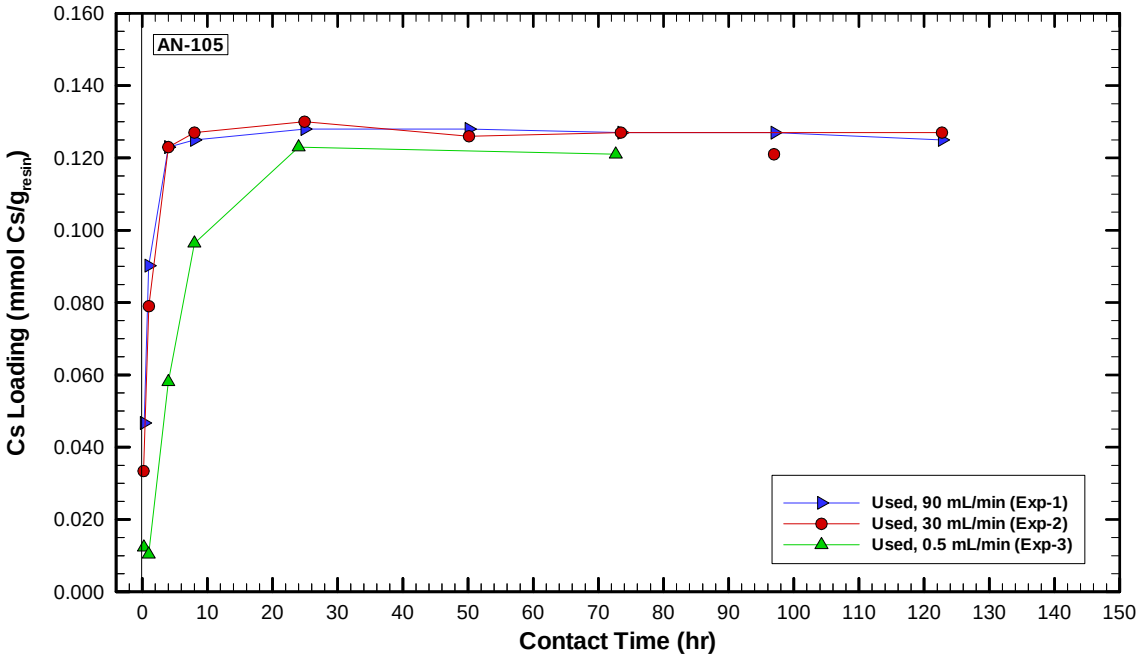

Figure 4-5. Comparison of transient Cs loading levels at various flow rates.

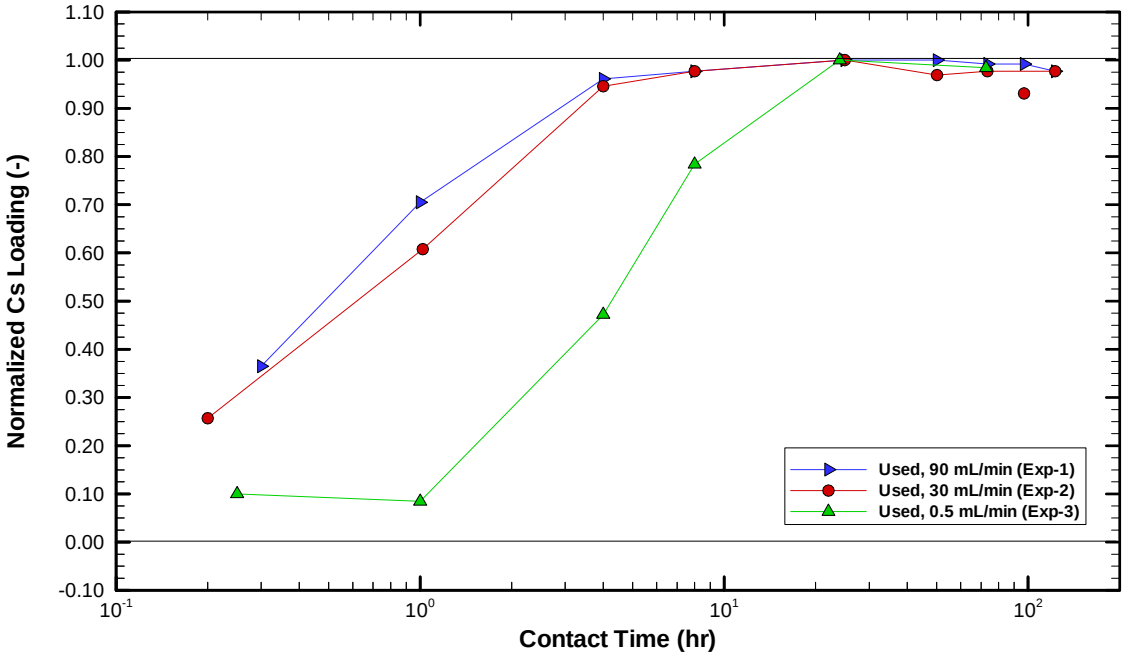

Figure 4-6. Comparison of normalized transient Cs concentration levels at various flow rates.

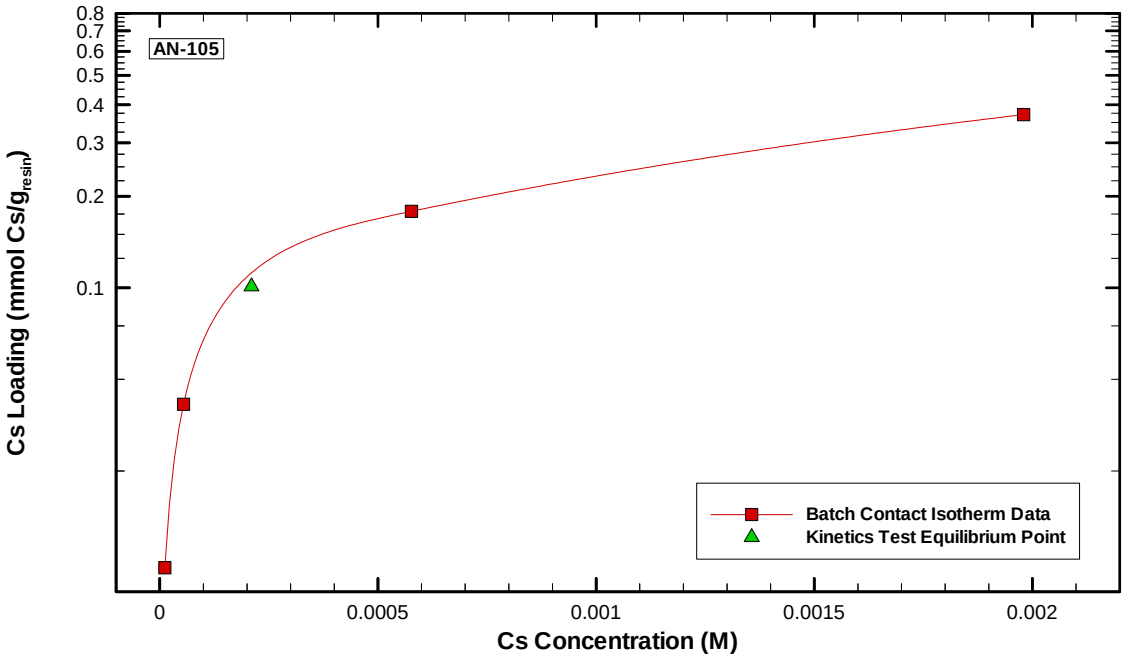

Figure 4-7. Cs sorption isotherm for spherical RF resin with baseline AN-105.

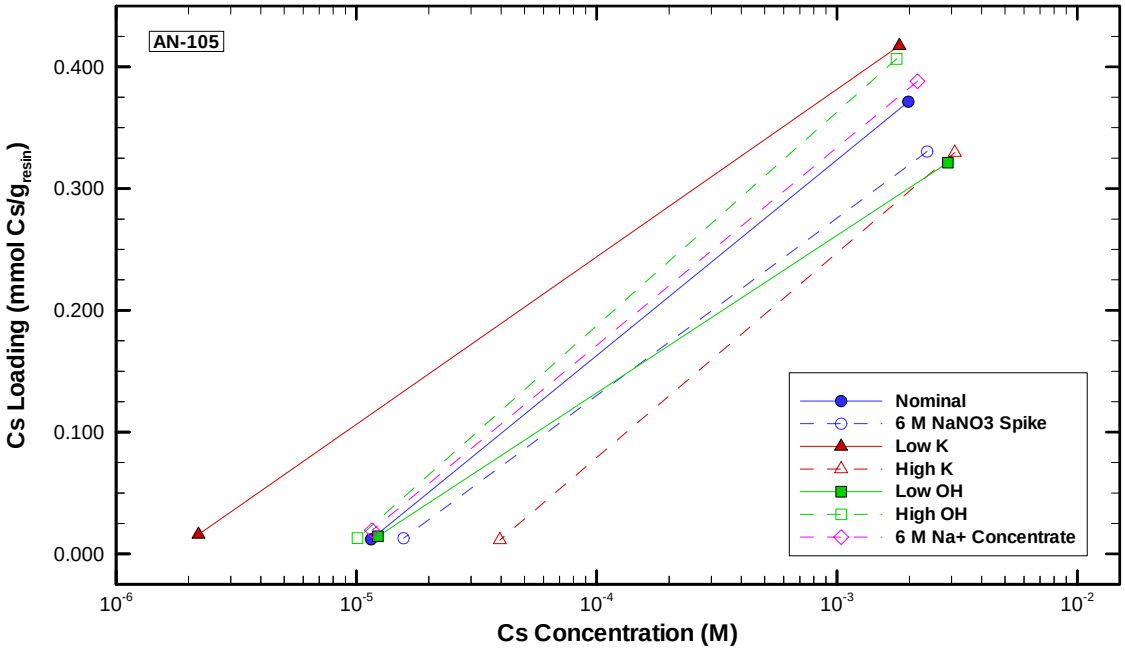

Figure 4-8. Cs isotherm endpoint data for spherical RF resin using modified AN-105 simulants.

5.0 Conclusions

- Temperature dependent cesium loading kinetics testing was performed at 25 and 45 °C using used spherical RF resin and baseline Envelope A (AN-105) simulant (Batch 2). As expected, the adsorption capacity of the resin drops at higher temperatures. A drop in capacity of approximately 17% (+/- 5%) was observed when the temperature was increased from 25 to 45 °C. In addition, particle kinetics were faster at higher temperatures which was also expected. A decrease in the apparent capacity of approximately 8% was observed between the 8- and 72-hour samples in the 45 °C test. This may indicate degradation of the resin at elevated temperatures.

- Particle type dependent kinetics testing was performed with "used" spherical, "unused" spherical and granular RF and baseline Envelope A (AN-105) simulant (Batch 2). The rate of uptake and capacity for the "used" and "unused" spherical resins were virtually identical. The Cs loading rate for the spherical resin is slightly greater than that of the granular resin, with the granular exhibiting a greater capacity by approximately 16% (+/- 5%) at the same initial concentration of 6.65 μg Cs/L (average).

- Flow rate dependent kinetics testing was performed with "used" spherical RF resin, baseline Envelope A (AN-105) simulant (Batch 1), and flow rates of 0.5 mL/min (0.208 cm/min), 30 mL/min (12.5 cm/min), and 90 mL/min (37.5 cm/min). As expected, the adsorption capacity of the resin was independent of the flow rate.

- The cesium loading isotherm for "used" spherical RF resin was obtained by batch contact testing with the baseline AN-105 simulant. The cesium capacity of spherical RF resin (~0.5 mmol Cs/g resin) in this matrix is ~90% (sodium form dry mass basis) of the capacity observed for SuperLig® 644 resin. The relative shapes of the loading isotherms for these two materials under the same conditions indicate that RF resin is less selective for cesium than SuperLig® 644 resin over other competitors.

- Isotherm endpoint data was obtained for various modified AN-105 simulants to evaluate the impact of competitors on cesium sorption. General trends in the data are consistent with those observed for SuperLig® 644 resin with cesium loading varying in the sequence: high K^+ < high Na^+ ≅ Low OH^- < nominal < high OH^- < low K^+.

6.0 References

Abodishish, H., 2003. "Batch Equilibrium and Particle Kinetics Tests for RF Resin", 24590-PTF-TSP-RT-03-0006, June.

Duffey, C. E., L. L. Hamm, W. D. King, 2003a. "Determination of Perrhenate (ReO_4^-) Absorption Kinetics from Hanford Waste Simulants Using SuperLig® 639 Resin", WSRC-TR-2002-00548, (SRT-RPP-2002-00272).

Duffey, C. E., W. D. King, 2003b. "Task Technical and Quality Assurance Plan for Batch Equilibrium and Particle Kinetics Tests for RF Resin", WSRC-TR-2003-00257, (SRT-RPP-2003-00122), July 17.

Eibling, R. E., C. A. Nash, 2001. "Hanford Waste Simulants Created to Support the Research and Development on the River Protection Project – Waste Treatment Plant", Westinghouse Savannah River Company document, WSRC-TR-2000-00338 (SRT-RPP-2000-00017), Rev. 0, February.

Fiskum, S. K., et al, 2004. "Comparison Testing of Multiple Resorcinol-Formaldehyde Resins for the River Protection Project – Waste Treatment Plant", WTP-RPT-103, Rev 0, January.

German, R. M., 1989. Particle Packing Characteristics, Metal Powder Industries Federation, Princeton, p. 106.

Hamm, L. L., F. G. Smith, D. J. McCabe, 2000. "Preliminary Ion Exchange Modeling for Removal of Cesium from Hanford Waste Using SuperLig® 644 Resin", BNF-003-98-0220, Rev. 0, June 16.

Hamm, L. L., S. E. Aleman, B. J. Hardy, C. E. Duffey, W. D. King, 2004. "Ion Exchange Modeling for Removal of Cesium from Hanford Waste Using SuperLig® 644 Resin", WSRC-TR-2003-00555 (SRT-RPP-2003-00242), Rev. 0, May.

Hassan, N. M., K. Adu-Wusu, 2003. "Cesium Removal for Hanford Tank 241-AW-101 Supernate Using Resorcinol-Formaldehyde Resin (U)", Westinghouse Savannah River Company document, WSRC-TR-2003-00433 (SRT-RPP-2003-00224), December.

Steimke, J. L., 2003a. "Hanford RPP-WTP SL-644 Program –Protocol P1: Resin Removal from Buckets, Resin Pretreatment and Resin Loading to Column", SRT-RPP-2003-0048.

Steimke, J. L., 2003b. "Hanford RPP-WTP SL-644 Program –Protocol P4: Measurement of Column Resin Dry Mass Basis", SRT-RPP-2003-0049.

Thorson, M. R., 2003. "Develop Requirements for Resorcinol Formaldehyde Alternate Resin", 24590-PTF-TSP-RT-02-016.

(This Page Intentionally Left Blank)

Appendix A. Analytical Results

Table A-1. Analytical results and masses for individual samples used for batch contact testing.

ADS#	Sample ID[a]	Resin Wt. (g)	Solution Wt. (g)	Solution Vol. (mL)	Phase Ratio (mL sol./ g resin)	[Cs] (ug/L)	Description
201146	A	1.0676	123.0379	100.4	94.1	7.19E+03	Base AN-105/Nom. Cs
201147	A-D	1.0695	123.0473	100.4	93.9	7.28E+03	Base AN-105/ Nom. Cs
2001154	A-FD	---	---	---	---	6.58E+04	Base AN-105/ Nom. Cs
2001155	A-FD-D	---	---	---	---	6.57E+04	Base AN-105/ Nom. Cs
2001148	B	1.0687	123.1358	100.5	94.1	2.56E+05	Base AN-105/ Nom. Cs
2001149	B-D	1.0707	123.013	100.4	93.8	2.69E+05	Base AN-105/ Nom. Cs
2001156	B-FD	---	---	---	---	7.77E+05	Base AN-105/ Nom. Cs
2001157	B-FD-D	---	---	---	---	7.99E+05	Base AN-105/ Nom. Cs
2001150	C	1.0678	123.0261	100.4	94.1	7.71E+04	Base AN-105/Interm. Cs
2001151	C-D	1.0694	123.1089	100.5	94.0	7.64E+04	Base AN-105/ Interm. Cs
2001158	C-FD	---	---	---	---	3.22E+05	Base AN-105/ Interm. Cs
2001159	C-FD-D	---	---	---	---	3.36E+05	Base AN-105/ Interm. Cs
2001152	D	1.0683	123.0237	100.4	94.0	1.55E+03	Base AN-105/Low Cs
2001153	D-D	1.0660	123.1263	100.5	94.3	1.51E+03	Base AN-105/Low Cs
2001160	D-FD	---	---	---	---	1.85E+04	Base AN-105/Low Cs
2001161	D-FD-D	---	---	---	---	1.85E+04	Base AN-105/Low Cs
201138	B	0.9777	121.9431	99.5	101.8	2.68E+05	Base AN-105/High Cs
201139	B-D	0.9794	121.6819	99.3	101.4	2.70E+05	Base AN-105/High Cs
201144	B-FD	---	---	---	---	8.04E+05	Base AN-105/High Cs
201145	B-FD-D	---	---	---	---	7.80E+05	Base AN-105/High Cs
2001152	D	1.0683	123.0237	100.4	94.0	1.55E+03	Base AN-105/Low Cs
2001153	D-D	1.0660	123.1263	100.5	94.3	1.51E+03	Base AN-105/Low Cs
2001160	D-FD	---	---	---	---	1.85E+04	Base AN-105/Low Cs
2001161	D-FD-D	---	---	---	---	1.85E+04	Base AN-105/Low Cs
202803	E	0.9587	123.0110	98.7	103.0	3.95E+05	Low OH/High Cs
202804	E-D	0.9586	123.1078	98.8	103.1	3.72E+05	Low OH/High Cs
202805	E-FD	---	---	---	---	7.92E+05	Low OH/High Cs
202806	E-FD-D	---	---	---	---	8.04E+05	Low OH/High Cs
202807	F	0.9600	123.1039	98.8	102.9	2.44E+03	Low OH/Low Cs
202808	F-D	0.9593	123.0241	98.7	102.9	2.47E+03	Low OH/Low Cs
202809	F-FD	---	---	---	---	2.09E+04	Low OH/Low Cs
202810	F-FD-D	---	---	---	---	2.11E+04	Low OH/Low Cs

[a] D indicates duplicate samples; FD indicates liquid feed samples

Table A-1. (continued)

ADS#	Sample ID[a]	Resin Wt. (g)	Solution Wt. (g)	Solution Vol. (mL)	Phase Ratio (mL sol./ g resin)	[Cs] (ug/L)	Description
201166	G	1.0059	123.0735	100.9	100.3	2.35E+05	High OH/High Cs
201167	G-D	1.0089	123.0841	100.9	100.0	2.36E+05	High OH/High Cs
201172	G-FD	---	---	---	---	7.75E+05	High OH/High Cs
201168	H	1.0079	123.0992	100.9	100.1	1.34E+03	High OH/Low Cs
201169	H-D	1.0068	123.0350	100.8	100.2	1.34E+03	High OH/Low Cs
201173	H-FD	---	---	---	---	1.84E+04	High OH/Low Cs
201174	I	1.0070	123.0781	101.0	100.3	2.37E+05	Low K/High Cs
201175	I-D	1.0091	123.1513	101.0	100.1	2.46E+05	Low K/High Cs
2001182	I-FD	---	---	---	---	7.95E+05	Low K/High Cs
2001176	J	1.0095	123.1221	101.0	100.1	5.96E+02	Low K/Low Cs
2001177	J-D	1.0083	123.1106	101.0	100.2	5.81E+02	Low K/Low Cs
201183	J-FD	---	---	---	---	2.17E+04	Low K/Low Cs
201178	K	1.0070	123.1174	97.6	97.0	4.02E+05	High K/High Cs
201179	K-D	1.0073	123.0521	97.6	96.9	4.20E+05	High K/High Cs
201184	K-FD	---	---	---	---	8.63E+05	High K/High Cs
201180	L	1.0079	123.0754	97.7	96.9	5.17E+03	High K/Low Cs
201181	L-D	1.0088	123.2022	97.8	96.9	5.33E+03	High K/Low Cs
201185	L-FD	---	---	---	---	2.10E+04	High K/Low Cs
201186	M	1.0092	123.0504	97.0	96.2	2.91E+05	6 M Na^+ Conc./High Cs
201193	M-D	1.0074	123.0422	97.0	96.3	2.83E+05	6 M Na^+ Conc./High Cs
201220	M-FD	---	---	---	---	8.23E+05	6 M Na^+ Conc./High Cs
201194	N	1.0093	123.0409	97.0	96.1	3.05E+03	6 M Na^+ Conc./Low Cs
201195	N-D	1.0074	123.0158	97.0	96.3	3.07E+03	6 M Na^+ Conc./Low Cs
201201	N-FD	---	---	---	---	2.98E+04	6 M Na^+ Conc./Low Cs
201196	O	1.0068	123.0443	97.2	96.5	3.18E+05	6 M Na^+ Spike/High Cs
201197	O-D	0.9358	114.0687	90.1	96.3	3.11E+05	6 M Na^+ Spike/High Cs
201202	O-FD	---	---	---	---	7.70E+05	6 M Na^+ Spike/High Cs
201198	P	1.0090	123.0758	97.3	96.4	1.86E+03	6 M Na^+ Spike/Low Cs
201199	P-D	1.0087	123.0760	97.3	96.5	2.31E+03	6 M Na^+ Spike/Low Cs
201203	P-FD	---	---	---	---	2.00E+04	6 M Na^+ Spike/Low Cs
201204	P-FD-D	---	---	---	---	2.00E+04	6 M Na^+ Spike/Low Cs

[a] D indicates duplicate samples; FD indicates liquid feed samples

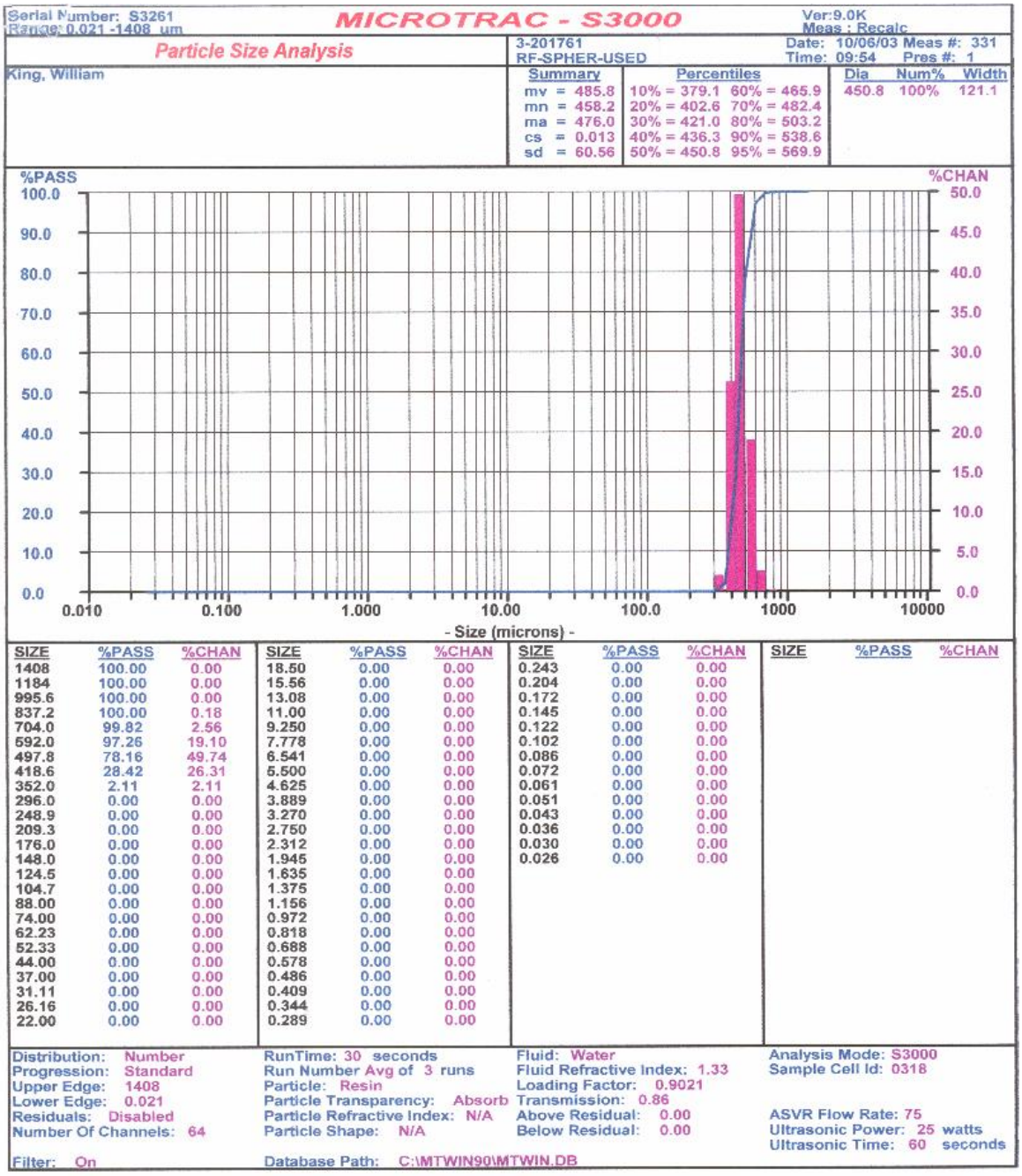

Figure A-1. Microtrac® particle size analysis data for the spherical RF sample (number-based data).

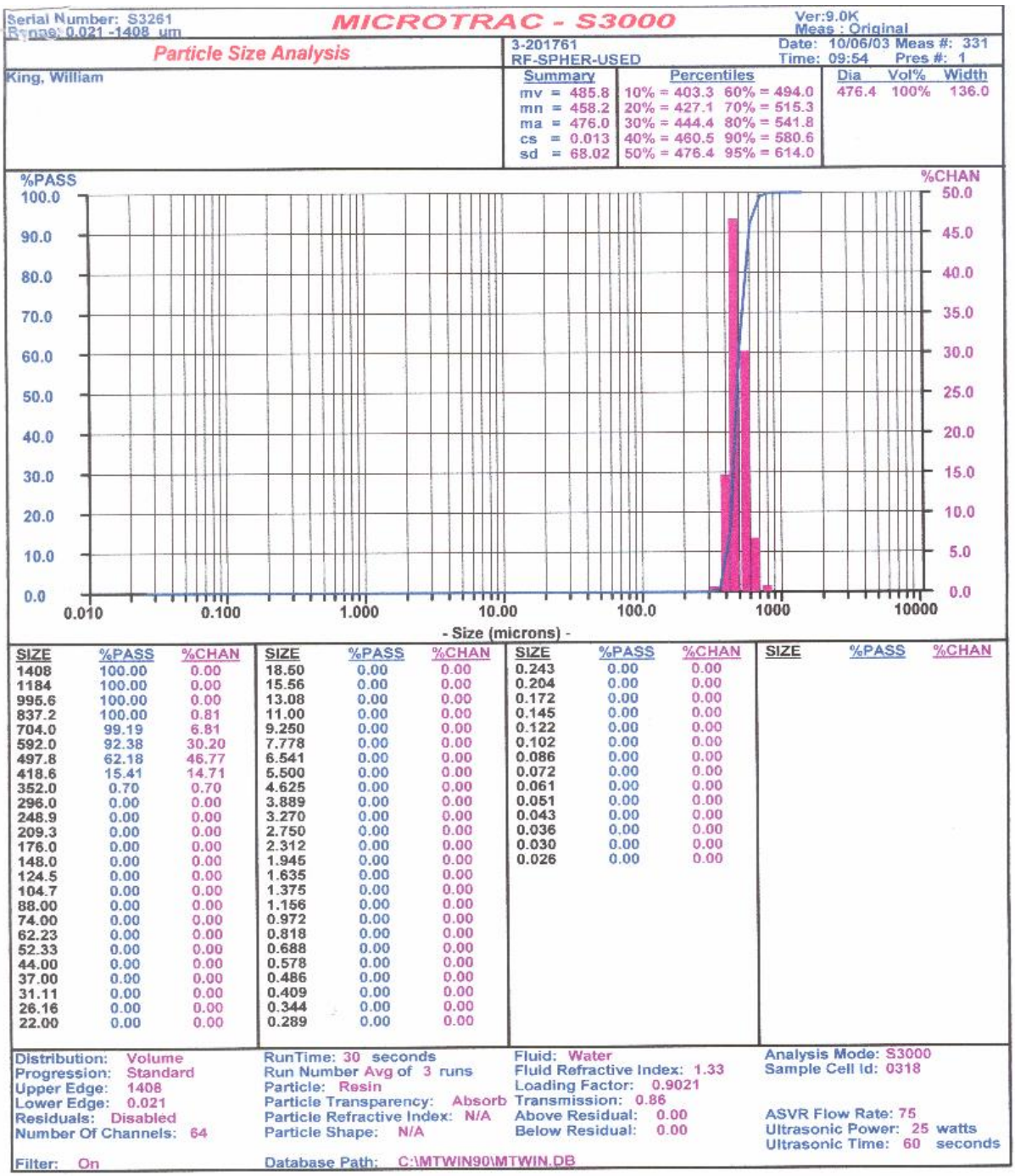

Figure A-2. Microtrac® particle size analysis data for the spherical RF sample (volume-based data).

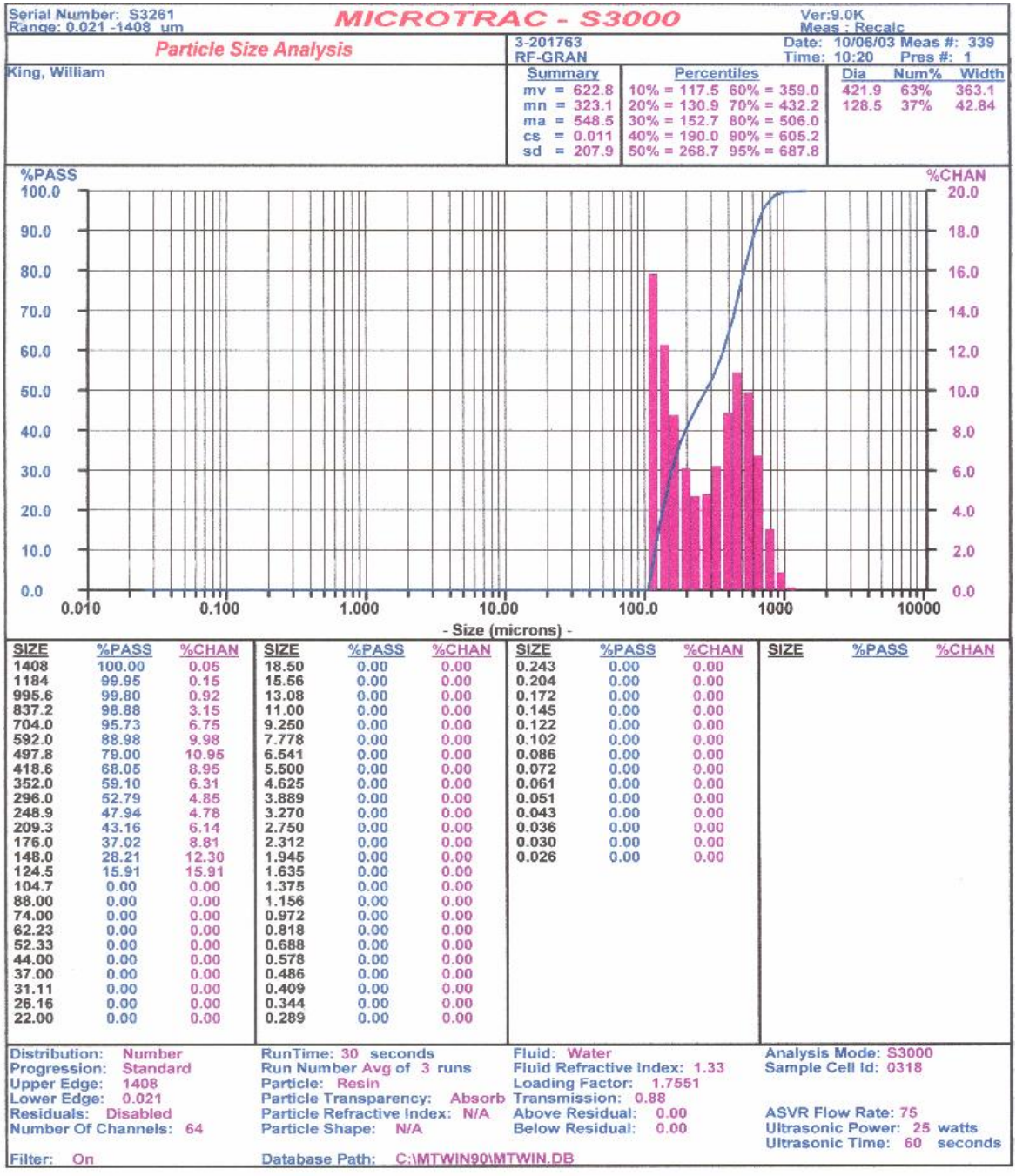

Figure A-3. Microtrac® particle size analysis data for the granular RF sample (number-based data).

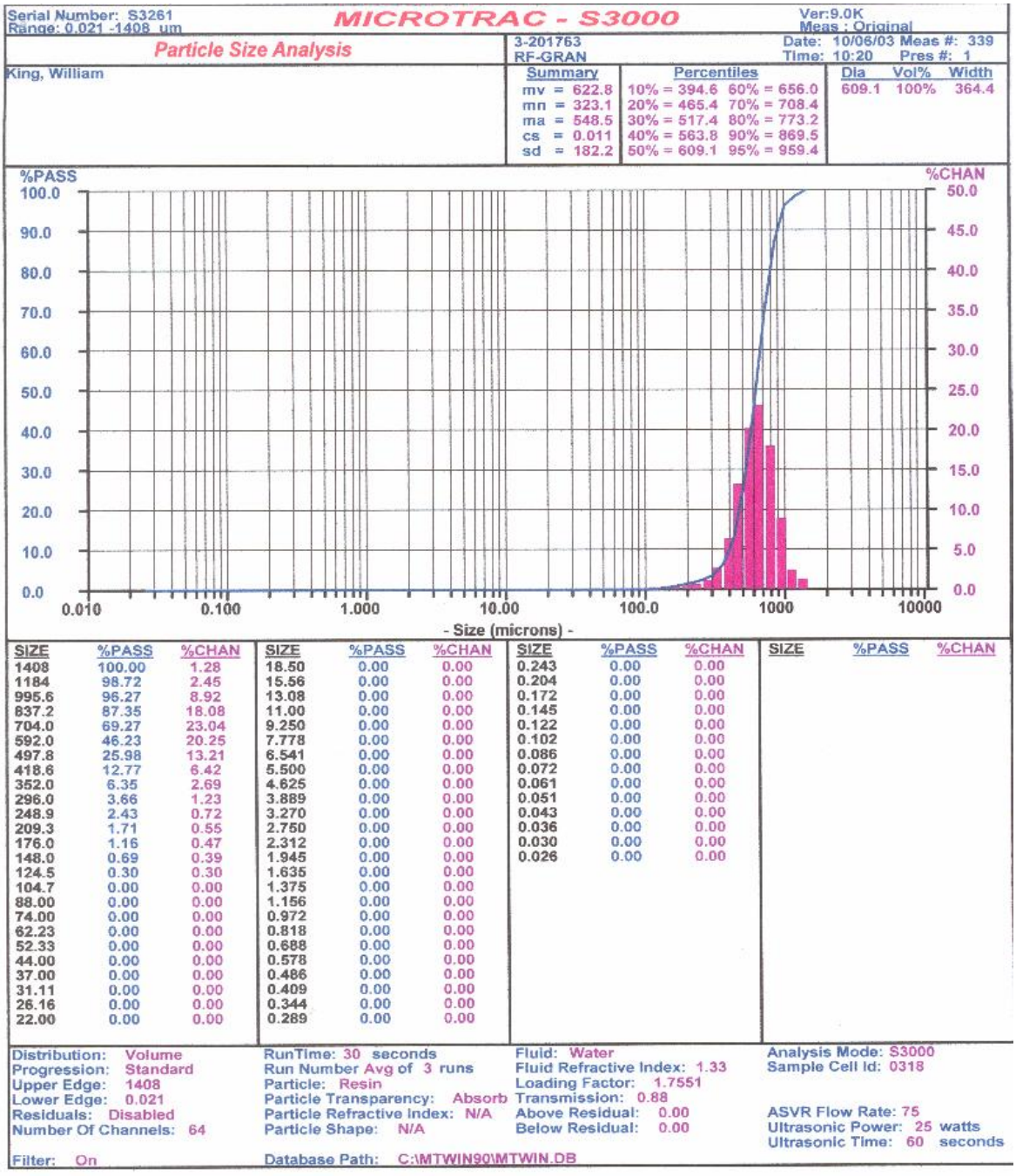

Figure A-4. Microtrac® particle size analysis data for the granular RF sample (volume-based data).